BSc Thesis Applied Physics and Applied Mathematics

Entanglement entropy for 2D spin lattices

Alexander S. Ivlev
Student Number: 4545729

Delft University of Technology

Supervisors

Prof. dr. Y.M. Blanter — Dr. P.M. Visser

Committee Members

Dr. M. Blaauboer — Dr. W.G.M. Groenevelt

Faculty of Applied Sciences — DIAM

July 11, 2019 — Delft

Contents

Abstract

This thesis will focus on verifying the area-law for the entanglement entropy S_N for spin-$\frac{1}{2}$ lattice systems in 2 dimensions, with ferromagnetic interactions defined by the nearest neighbour XX-model. The area-law implies that the S_N of a subsystem is expected to scale proportionally to the size of the boundary through which that subsystem interacts with the rest of the system. By writing a numerical model in MATLAB, which uses computational devices to circumvent the huge memory requirement that quantum simulations usually demand, it is possible to analyse 2 dimensional systems up to a lattice size of 5×5 for the first time. These finite systems have been assigned periodic boundary conditions, as if it were a torus. It doesn't seem possible to evaluate such systems analytically, unlike 1 dimensional systems, as we will show.

To test the area-law, it is first needed to calculate the systems groundstate. After all, it is predicted that the area-law is only followed by states near the groundstate. It is shown that the groundstate eigenvector for the Ising-model Hamiltonian, on which the system is based, can be determined to high accuracy with computational methods. The standard deviation in the calculated eigenvalue is in the order of numerical precision $\sigma_{GS} = 10^{-8}$, with the exact values depending on the system sizes. These groundstates are calculated for different external magnetic fields and a constant ferromagnetic coupling.

The groundstates are subsequently used to calculate the entanglement entropy as function of square subsystem boundary, and based on the first non-zero datapoint a line plotted through this data. This linear function corresponds exactly to the area-law in 2 dimensions. For subsystems up to approximately half the size of the total system the area-law gives a good approximation. Whenever the subsystem approaches the boundary, the entropy is beneath the area-law prediction. This seems results from the periodic boundary conditions, which produce an additional self-interaction of the subsystem through the boundary. That hypothesis is backed-up by the fact that if the total system is larger, the linear relation is upheld for longer and works better for the same subsystem. The linear fit namely produces a coefficient of determination $R^2 = 0.9782$ for 5×5 systems in comparison to $R^2 = 0.8593$ for 4×4 systems. Next to that, it should be noted that the area-law is not followed by excited states, which grow more than linearly when the system is smaller than the boundary. It could be concluded, while being cautious due to a lack of data-points, that the area-law is verified by these observations.

To check this a final time, the spin correlation $\langle \sigma_i^z; \sigma_j^z \rangle$ of the different particles is analysed. It is known from theory that, whenever this spin-correlation decays exponentially with distance, an area-law is present. Now due to the periodic boundaries, it has been conceived to not just fit the exponential decaying function, but to extend this function periodically. It has been analytically shown, that a repeating decaying exponential, behaves locally like a hyperbolic cosine. This hyperbolic cosine is fitted to the correlation in 5×5 systems, which produced a highly accurate fit with a coefficient of determination $R^2 = 0.9846$ and a correlation length of $\xi = 0.462 \pm 0.001$. This high accuracy and low standard deviation point to the fact that this periodic decaying exponential is a good approximation of the data, and thus the theory behind it is verified to a large extent. Thus it is indeed necessary to include the periodic bounds in the analysis, which explains the apparent violation of the area-law for large subsystems, and the correlation decays periodically indeed. It can be concluded that the linear area-law is indeed upheld for the 2 dimensional quantum systems near the groundstate.

More research is advised to check these relations in even bigger systems for better area-law verification. It is also interesting to analyse at what point the statevectors no longer follow the area-law, how distinct they should be from the groundstate. Quantifying this phase-transition is bound to give a better understanding of the behaviour. Next, one should analyse the behaviour for non-square subsystems. Finally, while the effect of varying magnetic fiels is analysed in this paper, more research on that front can be done, as well as different alterations to the Hamiltonians coupling constants. The numerical code allows for this dynamic, and could be interesting to follow as a research direction.

1 Introduction

The subject of Quantum Mechanics is one of the most important ones in modern physics. Due to the beauty of the theory, its mathematical rigour, and the unprecedented predictive power it provides, it is widely regarded as the single most fundamental theory. Even Einstein's marvelous theory of general relativity is seen as a temporary result that will probably be replaced by a quantum mechanical counterpart. Studying quantum mechanics therefore means studying reality.
Due to the importance of quantum, the field is extremely wide, with many different directions of research. One of those directions is Quantum Information. In the contemporary quantum mechanics, it is understood that information plays a key -if not the main- role. It was no surprise that the most famous modern dispute between the greats of the time, dubbed the 'Black Hole War' between Leonard Susskind and Stephan Hawking, focused on information. The quantum information paradox at the core of this dispute remains unsolved to this day.
To understand quantum information it is necessary to study quantum entanglement entropy, which is a measure of how much quantum information about its surrounding is stored in a certain system. From black-hole physics it is known that this quantum entropy has a somewhat peculiar behaviour, as it scales with the boundary area of a system. This means that the information that can be stored in a system is as large as its boundary area, while one could expect this to be as large as its volume. This gives room to wild and interesting theories, like the holographic principle and the related Anti-de Sitter/Conformal Field Theory correspondence.
Next to black holes, this area-law seems to hold for the ground-states of spin systems. The main focus of previous research has been the 1 dimensional spin-systems, which have been solved analytically. The area-law has been found there up to a logarithmic correction factor. This logarithmic correction is expected to provide a good bound in higher dimensions as well under certain conditions. If it is indeed the case that the area-law holds for higher-dimensional systems, it has among other things the potential to reduce the complexity of many-particle systems.

This thesis will focus on verifying the area-law for quantum entanglement entropy in 2 dimensional spin-$\frac{1}{2}$ lattice systems with periodic boundary conditions. For this the groundstate of systems up to the size of 5×5 particles is computed for a ferromagnetic, nearest neighbour, XX-model Hamiltonian. After this the entanglement entropy of square subsystems is computer and compared to a linear area-law function. Also the correlation between particles is analysed as function of their distance, as this also indicates the existence of an area-law.
After the list of variables, chapter 3 will discuss general quantum mechanical theory, the very basics of the subject. Chapter 4 will focus on quantum entanglement entropy which is needed to understand the theory of the thesis. Next, chapter 5 will discuss the model, on which the numerical simulation of the thesis is based, and derive the analytic solution for 1 dimensional periodic systems. We will try to apply this analytic approach (unsuccessfully) to 2D systems, to show the need for a numerical simulation. This simulation is described in detail in chapter 6. The results will be presented in chapter 7. Finally these results will be discussed and a conclusion is drawn from them in chapters 8 and 9 respectively.

2 List of Variables

Symbol	Description
A	Oftentimes used to denote a **subsystem** of particles.
B	Oftentimes used to denote the complement of a **subsystem** A of particles, inside the total system.
$\mathcal{H}_A$	**Hilbert Space** for system A of some dimension.
$\|\psi\rangle \in \mathcal{H}$	**Wavevector** or **statevector** in the Hilbert Space $\mathcal{H}$. This is a pure quantum state.
$\|\psi(\vec{r})\rangle$	The wavevector represented in Eucledian space.
$\hat{O} \in B(\mathcal{H})$	An **operator** on the Hilbert Space, each operator is an element of the C^*-algebra of bounded linear operators.
ρ_{AB}	The **density operator** in the C^*-operator-algebra of some state in the Hilbert space $\mathcal{H}_\mathcal{A} \otimes \mathcal{H}_\mathcal{B}$.
$S_N(\rho_A)$	**Von Neumann Entropy** of a state discribed by the density operator ρ_A, which is also referred to as quantum entanglement entropy.
$S_N(A)$	Von Neumann Entropy of system A. In this paper A will always refer to a collection of fermions in a lattice.
$\partial(I)$	**Boundary** of a the system I.
$\langle \hat{A}_i; \hat{A}_j \rangle$	The **connected correlation** between the particels i and j for the quantities measured by the Hermitian operator $\hat{A}$.
ξ	**Correlation length**, a parameter used to describe the correlation between two particles at a certain distance.
$d(i,j)$	The **distance** between particles i and j as measured by some metric.

3 Quantum Theory

In this section some essential background of Quantum Mechanics that is necessary to understand the paper will be provided. It will include a overview of standard Quantum Mechanical properties like superposition, entanglement as well as slightly more advanced structures like density matrices. Additionally it will be shown how these structures are manipulated in the framework of linear algebra. The reader particularly familiar with Quantum-Mechanics should feel free to skip ahead, however it should be noted that the notations introduced in this section could be used in the remainder of the paper.

3.1 Quantum States, Hilbert Spaces and Operators

As is probably familiar to any reader, the theory of Quantum Mechanics is a theory concerning the very small. It was originally kick-started by Max Planck, who solved the Ultra-Violet Catastrophe by assuming that light radiation can be absorbed and emitted in discrete packets depending on it's frequency [1]. This theory was further progressed by great minds like Albert Einstein, Niels Bohr, John Von Neumann, Erwin Schrödinger and many others [2–5]. The understanding, by the leading Copenhagen-interpretation of Bohr and Heisenberg [6], is that the Quantum Mechanical particles are in an non-deteministic state before they are measured by an observer. This means that the exact state of the particle that will be measured isn't known from the start, but is a probability distribution given by the absolute squared $|\psi|^2$ of the so called wave-function of the particle, Whenever this wavefunction is projected on a certain basis. As an example, the probability distribution of the particle in the basis associated with space is $\langle\psi|\,|\vec{r}\rangle\langle\vec{r}|\,|\psi\rangle$, where $|\vec{r}\rangle\langle\vec{r}|$ is the projection matrix on to Euclidean space[1], the exact notation will be made clear later in this chapter. This wave-function is also often called the statevector, since it is mathematically described as a vector in a complex Hilbert space $|\psi\rangle \in \mathcal{H}$. The brackets are a convention and useful to make this distinction very clear. This Hilbert space can be of any dimension, depending on the exact system. Formally speaking a Hilbert space is a complex inner product space which is complete under the metric induced by the inner product. Further details about these properties of Hilbert spaces are not necessary to discuss for the comprehension of the paper, but can be found in [7].

The behaviour of the wavevector $|\psi\rangle$ over time is described by the so-called 'time-dependent' Schrödinger Equation. This is the differential equation is given by (1):

$$i\hbar\frac{\partial}{\partial t}\,|\psi(\vec{r},t)\rangle = \hat{H}(\vec{r},t)\,|\psi(\vec{r},t)\rangle \tag{1}$$

where $\hbar$ is the reduced Planck Constant, $\hat{H}$ is the Hamiltonian of the system with the hat making it clear that it an operator (the details of which will be discussed later), and $\vec{r}$ is the position in our usual Euclidean space. More specifically, this formula describes how the statevector in the Hilbert Space behaves in time when it is represented in Euclidean space.
Let us quickly focus our attention on the Hamiltonian. The Hamiltonian is an operator used to determine the energy of the statevector, or rather the possible energies since the the energy of the statevector are indetermined before measurement. It is no coincidence that the operator that determines energy is responsible for the time-evolution of the state by the Schrödinger Equation (1). After all, by Noether's Theorem [8] the fact that energy is a conserved quantity under time-translation, the Hamiltonian must be the generator of the time-evolution. Just as in classical mechanics, the Hamiltonian is given by the sum of the kinetic energy $\hat{K} = \frac{\hat{p}^2}{2m}$, with $\hat{p}$ the momentum operator and m the mass of the system, and the potential energy $\hat{V}(\vec{r},t)$. The potential depends on the system that is described and is often dependent of the position and can be dependent on the time. For our purposes in this paper kinetic energy is not of interest as we will consider static particles in a lattice that have no relative motion.

[1] Or actually a infinitely dimensional operator, whose notation is abused a little

Therefore it will not be discussed further. For additional readings, on kinetic energy and the momentum operator $\hat{p}$, one can refer the usually mentioned book by Griffiths [9].
For mathematical formality, however, a final note on operators will be made. Linear operators in quantum mechanics, of a Hilbert space $\mathcal{H}$, are formally elements of the algebra of bounded linear operators on the Hilbert Space $B(\mathcal{H})$. This algebra is a C^*-algebra, in fact every C^*-algebra is isomorphic up to conjugation to such an algebra of bounded linear operators, by the Gelfand–Naimark theorem [10]. So an operator $\hat{A} \in B(\mathcal{H}) : \mathcal{H} \to \mathcal{H}$ is a linear bounded operator from the Hilbert space to itself. Additionally, Hermitian operators $\hat{A} = \hat{A}^*$ correspond to observable physical quantities.

3.2 Eigenvectors, inner product and probability of states

Now that Hilbert spaces, statesvectors and operations are covered, it is important to discuss what these statevectors mean and how they are used to interpret physical quantities. As mentioned above, the quantum-mechanical state is non-deterministic when performing a measurement of an observable quantity. These observable quantities are described by the corresponding Hermitian operators. Now the probability that a certain quantity is measured, can be determined by rewriting the state as a decomposition into eigenvectors $|\phi_n\rangle$ of the corresponding operator:

$$|\psi\rangle = \sum_{n=1}^{dim(\mathcal{H})} c_n \, |\phi_n\rangle \tag{2}$$

The decomposition coefficients c^n are given, as usual, by the inner product denoted as $\langle\phi_n|\psi\rangle$ [9]. The absolute squared value of these coefficients $|c_n|^2$ gives the probability of measuring the corresponding eigenvalue λ_n. For this to hold it is necessary that the statevector is normalized under the L_2-norm and that the eigenvectors used in the decomposition are also normalized. Since only the absolute value is important and the state is normed for any measurements and operations, it can be noted that the eigenvectors need technically not be elements of the Hilbert space $\mathcal{H}$ but merely an element of the Projective Hilbert space $P(\mathcal{H})$ of equivalence classes.
As an extra note, the inner product can also be viewed as multiplication of a covector $\langle\psi_i| \in \mathcal{H}^*$ and the vector $|\psi_j\rangle \in \mathcal{H}$ in Dirac bra-ket notation [9] where $\mathcal{H}^*$ is the dual-vectorspace of Hilbert space $\mathcal{H}$ such that all $\langle\psi| : \mathcal{H} \to \mathbb{C}$ are a bilinear form. For some orthonormal basis in the Hilbert space $|e_i\rangle$, there is a corresponding dual basis $\langle\varepsilon_i|$ such that $\langle\varepsilon_i|\epsilon_j\rangle = \delta_{ij}$.
Now that we know how to calculate the probabilities of measuring the eigenvalues corresponding to an operator, it is possible to determine the expectation value for measuring the quantity corresponding to that operator. This is simply the sum of the eigenvalues λ_n weighted by the probabilities $|c_n|^2$. So the expectation value of the the quantity A described by Hermitian operator $\hat{A} \in B(\mathcal{H})$ is given by $\langle A\rangle = \sum_{n=1}^{dim(\mathcal{H})} \lambda_n |c_n|^2$. It can be easily verified that $\langle A\rangle = \langle\psi| \, \hat{A} \, |\psi\rangle$ by writing $|\psi\rangle = \sum_{n=1}^{dim(\mathcal{H})} c_n \, |\phi_n\rangle$ with ϕ_n orthogonal the eigenvectors of $\hat{A}$ corresponding to eigenvalues λ_n, and c_n obviously $\langle\phi_n|\psi\rangle$.

3.3 Quantum Superposition

A useful and interesting property of quantum mechanical systems (not unique to the Copenhagen interpretation [11]) is that a quantum state can be in a linear superposition of other states. A state is said to be a superposition whenever it is described as a linear combination of basis-vectors. Now this isn't exciting by itself, since any statevector, which may be written as a linear combination, can also be written as a single vector in some other basis. The magic happens when there are clear distinct spaces, for example when considering a lattice of particles. In that case the basis is no longer completely arbitrary but says something about the relation of the particles. The total Hilbert space can be considered as a tensor product of the Hilbert spaces corresponding to the individual particles. Each basisvector of the total vectorspace can be written as a tensorproduct of the basisvectors for the individual Hilbert spaces. However, whenever one takes a superposition of state in that case, it could

be the case that the resulting state can not longer be written as a tensorproduct state. This will lead to the interesting property called quantum entanglement, but more on that in the next chapter.

3.4 Fermions

The majority of this thesis will focus on analysing systems consisting of particles called fermions [9]. These quantum-mechanical particles are generally defined in either of two ways. Firstly they are considered to be half-integer spin particles. Spin is a quantum-mechanical number connected to magnetic moment. Electrons are an example of spin-$\frac{1}{2}$ particles and are thus fermions. The second definition[2] of defining them is as indistinguishable particles whose wavefunction is anti-symmetric under exchange of two particles. To give an example let us have a system of N particles, each at position $\vec{r}_i$. The (time-independent) wavefunction of this system is written as $|\psi(\vec{r}_1, \ldots, \vec{r}_i, \ldots, \vec{r}_j, \ldots, \vec{r}_N)\rangle$. If the particles are fermions and we let any of them swap places, the wavefunction gains a negative vector:

$$|\psi(\vec{r}_1, \ldots, \vec{r}_i, \ldots, \vec{r}_j, \ldots, \vec{r}_N)\rangle = -\,|\psi(\vec{r}_1, \ldots, \vec{r}_j, \ldots, \vec{r}_i, \ldots, \vec{r}_N)\rangle$$

Similar negative factors are applied when some other transformation, that are usually considered symmetric, occur e.g. rotating the particle by 2π about it's own axis. Mathematicians tend to refer to these objects as 'spinors'.

In this thesis the focus will lie on the spin-$\frac{1}{2}$ electrons. It is useful to introduce some sort of notation for writing spin-$\frac{1}{2}$ particles. For this it is first needed to understand that quantum-mechanical spin is discrete, as one would expect for any quantity in quantum mechanics. Next to a value, the spin also has a directional component. While the total spin of a spin-$(k + \frac{1}{2})$ fermion is set in stone, namely $|k = \frac{1}{2}|$, the component of in the z-direction S_z, can be an integer away from the total while being absolutely smaller: $S_z \in \{-k - \frac{1}{2}, -k + \frac{1}{2}, \ldots, k - \frac{1}{2}, k + \frac{1}{2}\}$. The z-direction is chosen by definition. For an spin-$\frac{1}{2}$ particle like an electron, the z-component of the spin is either $\frac{1}{2}$ or $-\frac{1}{2}$. The two statevectors corresponding to these components span the complete Hilbert Space of the particle. The basevector corresponding to the $\frac{1}{2}$ or 'up' state is denoted as $|\uparrow\rangle$ and the $\frac{1}{2}$ or 'down' state as $|\downarrow\rangle$. A Hilbert Space consisting of multiple particles has basevectors that are the tensorproduct of these single-particle bases. For example $|\uparrow\uparrow\downarrow\uparrow\rangle \equiv |\uparrow\rangle \otimes |\uparrow\rangle \otimes |\downarrow\rangle \otimes |\uparrow\rangle$ is a basevector of a four particle system.

An important class of operators are the lowering a_i and raising $a_i^\dagger$ operators, or alternatively called the annihilation and creation operators. The subscript i denotes the basevector these operators act on. They are defined on fermions such that the annihilation operator turns a downstate into an upstate in some basis, and removes the upstates. The creation conversely turns the upstate into a downstate in some basis, and removes the downstates. These fermionic operators follow the canoncial anti-commutation relations:

$$\{a_l, a_m\} = \{a_l^\dagger, a_m^\dagger\} = 0 \qquad \text{and} \qquad \{a_l^\dagger, a_m\} = \delta_{lm} \tag{3}$$

Where $\{\cdot,\cdot\}{:}B(\mathcal{H}) \times B(\mathcal{H}) \to B(\mathcal{H})$ is defined as the bilinear form such that $\{a, b\} \mapsto ab + ba$.

3.5 Quantum Entanglement and Mixed States

A key concept of the paper is quantum entanglement and mixed states, therefore a recap on that matter is essential. Let's start with the former. Quantum entanglement always concerns multiple particles. We generally speak of particles to be entangled [12], whenever the total state of the system can not be described by individually looking at the states of the separate particles. The probability of one particle being in a specific state, depends on the state of the other particles. As an example think of a state with two spin-$\frac{1}{2}$ particles, A and B. Let the total normalized state be described by $|\psi\rangle = \frac{1}{\sqrt{2}}(|\uparrow_A\uparrow_B\rangle + |\downarrow_A\downarrow_B\rangle)$. Looking at the particles individually both would have a 50/50 chance of

[2] and in my opinion more elegant

being either up or down, but whenever we know that particle A is in state $|\uparrow\rangle$, by measuring it, we immediately change the probability distribution of B. In this case the state of B is completely known to be $|\downarrow\rangle$ and the system is called maximally entangled. A more quantitative description can be given after the concept of entropy is discussed, in the next section. The definition of entanglement can be made more more mathematically precise however. For that we first define a product state.

Definition. (Product State) Consider two Hilbert Spaces $\mathcal{H}_A, \mathcal{H}_B$ of dimension n, m. A state $|\psi\rangle_{AB} \in \mathcal{H}_A \otimes \mathcal{H}_B$ is a **product state** whenever there exist vectors $|\chi\rangle_A \in \mathcal{H}_A$ and $|\xi\rangle_B \in \mathcal{H}_B$ such that $|\psi\rangle_{AB} = |\chi\rangle_A \otimes |\xi\rangle_B$.

Obviously $|\chi\rangle_A$ and $|\xi\rangle_B$ can be written in terms of some basis. A state is called entangled, whenever it is no product state. Thus whenever there don't exist any $|\chi\rangle_A$ and $|\xi\rangle_B$ of such form.

Now we can move on to the concept of mixed states. A mixed state is a quantum state that can not be described by a single vector from the Hilbert Space at all. One can imagine this as inducing classical probabilities in the system, instead of a quantum probability distribution due to superposition.
Formally it is necessary to introduce the concept of density matrices. A density matrix, or density operator, is a way to represent the statistical distribution of the possible quantum states in the Hilbert space. The most general description of a density matrix ρ is:

$$\rho = \sum_i p_i \, |\psi_i\rangle\langle\psi_i| \tag{4}$$

where $|\psi_i\rangle$ are vectorstates from the Hilbert Space (thus pure-states), p_i give the classical probabilities and must sum to 1. Whenever such a density matrix is needed to describe the system, it can not be considered as a pure state but rather as a mixed state. As a note, this density operator is an element of the corresponding C^*-algebra as are the other operators.

One can construct a mixed state by creating an entangled state between Hilbert Spaces $\mathcal{H}_A, \mathcal{H}_B$ and ensuring that one of the Hilbert Spaces, say $\mathcal{H}_B$, is inaccessible to the observer. The state that still is accessible is called a mixed state. Mathematically speaking, let ρ_{AB} be the density matrix of the entangled state $|\psi\rangle \in \mathcal{H}_A \otimes \mathcal{H}_B$, thus $\rho_{AB} = |\psi\rangle\langle\psi|$. The inaccessibility of one part of the system is described by taking the partial trace over that part. A mixed state of the particles in the A space is denoted by the density matrix ρ_A created by taking the partial trace over the B-space $\mathrm{Tr}_B\{\cdot\}$, thus $\rho_A = \mathrm{Tr}_B\{\rho_{AB}\}$. Here the partial trace is defined as the linear and unique map such that: $\mathrm{Tr}_B\{\cdot\} : \mathcal{H}_A \otimes \mathcal{H}_B \to \mathcal{H}_A$ with $\rho_A \otimes \rho_B \mapsto \mathrm{Tr}\{\rho_B\}\rho_A$, where $\mathrm{Tr}\{\cdot\}$ is just the regular trace. This trace obviously is a linear mapping from a matrix to the sum of its eigenvalues, making the partial trace linear as well.
To show that this indeed a way to form mixed states, let us start with an entangled state $|\psi\rangle_{AB} \in \mathcal{H}_A \otimes \mathcal{H}_B$. By definition it can not be written as $\sum_i |\chi_i\rangle \otimes \sum_j |\xi_j\rangle$. By Schmidt Decomposition however, every state can be written as $|\psi\rangle_{AB} = \sum_i \alpha_i \, |\chi_i\rangle_A \otimes |\xi_i\rangle_B$ for some Schmidt coefficients α_i and some orthonormal basis $|\chi_i\rangle_A$ and $|\xi_i\rangle_B$. If this state is entangled, it can never be written with a single term in the sum. So there are at least two non-zero α_i. Then we have that $\rho_{AB} = \sum_{i,j} \alpha_i \bar{\alpha}_j \, |\chi_i\rangle\langle\chi_j| \otimes |\xi_i\rangle\langle\xi_j|$. When performing the partial trace on we get

$$\begin{aligned} \rho_A &= \mathrm{Tr}_B(\rho_{AB}) \\ &= \sum_{i,j} \alpha_i \bar{\alpha}_j \, |\chi_i\rangle\langle\chi_j| \, \mathrm{Tr}(|\xi_i\rangle\langle\xi_j|) \\ &= \sum_i |\alpha_i|^2 \, |\chi_i\rangle\langle\chi_i| \, \mathrm{Tr}(|\xi_i\rangle\langle\xi_i|) \end{aligned} \tag{5}$$

Since $|\xi_i\rangle$ is an orthonormal basis, we have trivially that $\mathrm{Tr}\{|\xi_i\rangle\langle\xi_i|\} = 1$. Thus we obtain

$$\rho_A = \sum_i |\alpha_i|^2 \, |\chi_i\rangle\langle\chi_i| \tag{6}$$

Whenever the state is entangled this density function has always multiple terms in the summand, and thus the resulting density matrix is a mixed state.

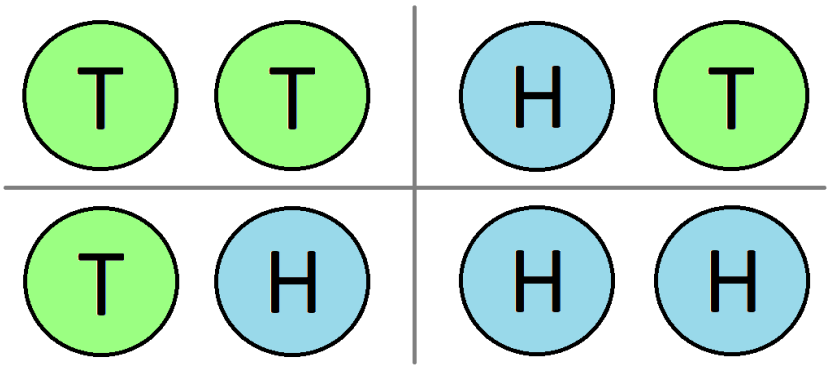

Figure 1: The possible coin-toss results when considering 2 coins. H displays heads and T displays tails. Since all the results, in case of a fair coin, are equal, the probability of each outcome is $p_i = \frac{1}{4}$. Using equation 7 one calculates $S = 2 \ln 2$.

4 Quantum Entanglement Entropy

This thesis concerns the concept of Quantum Entanglement Entropy and how it behaves in different systems. It is therefore essential for the understanding of the reading to dive into this subject, next to the basic quantum mechanics discussed in the previous section. First a review will be given of entropy in general, then how this is applicable to quantum entanglement. Furthermore the concept of the area-law is discussed, which describes the relationship in which the entropy increases as a function of the subsystem size. The connection of area-law to the so called correlation length is finally discussed.

4.1 Entropy

Classically the concept of entropy is used extensively in statistical thermodynamics and information theory. It has been originally proposed by Clausius and was further developed by Boltzmann, Gibbs and Shannon, among others [13–15]. From the perspective of information theory, entropy S quantifies the uncertainty of the state the system is in. If there are a larger number of possible states that a system is likely to occupy, the entropy is large. More specifically:

$$S = -\sum_i p_i \ln p_i \tag{7}$$

where p_i is the non-zero probability that the system is in state i. Note that this entropy is always positive since $0 \leq p_i \leq 1$, and the logarithm cancels the prefixed minus sign. Depending on the exact form of the equation and subject field it is discussed in, this is known as Gibbs Entropy or Shannon Entropy[3]. Whenever there are N total states, all of which have the probability $p_i = \frac{1}{N}$, the entropy is $S = \ln N$. Consider for example a (fair) coin that is tossed, but whose result is yet unknown. This system has finite entropy $S = \ln 2$, since there are two different possible positions the coin be in. If however 2 coins are tossed, the entropy $S = 2 \ln 2$ is substantially higher, as there is more possible positions for the system as seen in figure 1. A well-known generalization of the concept of entropy is Rényi Entropy [16], but this is beyond the scope of this thesis.

Entropy is of great theoretical importance in physics, since it seems to be the only mechanism dictating the flow direction of time. By the second law of thermodynamics, entropy must always increase in a isolated system, while other quantities like energy and momentum conserved. Thus

[3]This also depends whether you are talking to an engineer or mathematician. If you're uncertain, just refer to it as 'Entropy'. Whenever you are subsequently asked which one you mean, you know that you are talking to a physicist. In this case you can hopefully agree to use natural units resolving the problem altogether (up to a factor of $\ln 2 = 1$)

entropy is not symmetric under temporal inversion. In recent years more and more physicists have been suggesting that entropy, and the information that goes hand in hand with it, is one of the most fundamental quantities in physics. Some of them even proposed that it is the origin of the Gravitational Force [17]. These concepts go deeper than classical entropy however, they concern quantum entropy.

4.2 Quantum Entanglement Entropy

Now it is finally time to introduce Quantum Entanglement Entropy. As one would expect, this is the 'entropy' resulting from quantum entanglement. The formal definition of Quantum Entanglement Entropy used in this paper is due to Von Neumann [4] and will therefore sometimes be referred to as Von Neumann Entropy:

$$S_N(A) = -\operatorname{Tr}(\rho_A \ln \rho_A) \tag{8}$$

where ρ_A is the density matrix for system A and $\ln\{\cdot\}$ is the matrix logarithm.

Computing the matrix logarithm is a daunting task however, even if done numerically, and the concept of the logarithm of the density matrix may not be as intuitive. This can hinder the conceptual understanding of the subject for the reader[4]. Therefore it is useful to derive a more inviting form of Von Neumann Entropy, which resembles the classical from to an even greater extend:

$$S_N = -\sum_i \lambda_i \ln \lambda_i \tag{9}$$

where λ_i are the eigenvalues of the density matrix ρ from equation (8). Specifically, whenever $\lambda_i = 0$, this gives complications as equation (9) is undefined. In all cases we can take the limit of $\lambda \to \lambda_i$, or just take the non-zero eigenvalues. We can easily deduce (9) from (8) by diagonalizing the density operator $\rho = QDQ^*$, where D is diagonal and Q unitary. Now combining the expressions:

$$\begin{aligned}
\rho \ln \rho &= \rho \left((\rho - I) - \frac{(\rho - I)^2}{2} + \frac{(\rho - I)^3}{3} - ... \right) \\
&= QD((D - I) - \frac{(D - I)^2}{2} + \frac{(D - I)^3}{3} - ...)Q^* \\
&= QD \ln(D) Q^*
\end{aligned}$$

Since $\operatorname{Tr}(QD\ln(D)Q^*) = \operatorname{Tr}(Q^*QD\ln(D)) = \operatorname{Tr}(D\ln D)$, this directly produces equation (9), as we wished to show. For this derivation the power series of the matrix logarithm has been used. This power expansion is only applicable as long as $\|\rho - I\| < 1$. Let us show that this condition is indeed met. The matrix-norm $\|\cdot\|$ used here is the standard matrix norm such that $\|A\| = \sup_{|\vec{v}|=1} |A\vec{v}|$, with the standard Euclidean l_2 vector norm $|\cdot|$.
Now we know that $\rho = QDQ^*$. Thus

$$\begin{aligned}
\|\rho - I\| &= \|QDQ^* - QQ*\| \\
&= \|Q(D - I)Q^*\| \\
&\leq \|Q\|\|D - I\|\|Q^*\|
\end{aligned} \tag{10}$$

The last line holds for this norm. It simply has hold it since by the formal definition of the C^*-algebra, of which these operators are part, the C^* algebra is a Banach algebra. In any Banach Algebra, the elements follow this sub-multiplicative property that $\|AB\| \leq \|A\|\|B\|$. Now Q is an orthonormal matrix, so it consists of normed vectors that are orthogonal to each other and span the Hilbert space. After decomposing $\vec{v}$ into these orthonormal vectors, it is clear that the multiplication $Q^*\vec{v}$ will result in just a vector consisting of the decomposition coefficients. $Q^*\vec{v}$ is basically just a basis transformation, into the basis formed by the orthonormal vectors forming the columns of Q. $Q\vec{v}$ is the

[4] and for myself as well

reverse transformation. It is trivial that this will result in vectors such that $|Q^*\vec{v}| \leq 1$ and $|Q\vec{v}| \leq 1$ for any normed $\vec{v}$. So we have that:

$$\begin{aligned} \|\rho - I\| &\leq \|Q\|\|D - I\|\|Q^*\| \\ &\leq \|D - I\| \end{aligned} \tag{11}$$

Since $D - I$ is a diagonal matrix, and the diagonal entries of D are exactly the eigenvalues of ρ which we will see later obey the following conditions:

$$0 \leq \lambda_i \leq 1 \tag{12}$$

Therefore we have that the diagonal entries of $D-I$, κ_i, obey the condition $-1 \leq \kappa_i \leq 0$. Trivially this means that $\|D - I\| = \max_i \kappa_i$. We thus have that $\|\rho - I\| \leq 1$, which is not strictly smaller than 1, as the logarithmic expansion requires. Being strictily smaller is necessary, to prevent the singularities similar to $\ln(0)$. This however is not a problem in our case, as it only occurs if there are $\lambda_i = 0$. We can either choose to ignore as is done usually, or choose to take the limit $\tilde{\lambda}_i \to \lambda_i$, which does converge due to the linear term in front of the logarithm: $\lambda_i \ln(\lambda_i)$. So the inequality $\|\rho - I\| < 1$ either holds, or is an equility. In the latter case we can take the limit of the eigenvalues of ρ to go to zero or simply ignore them.

In order to gain a better understanding of the meaning of this Von Neumann entropy (9), we'll have to look at what the eigenvalues of the density matrix mean. Since the eigenvalues are the coefficients of the spectral decomposition $\rho = \sum_i p_i |\psi_i\rangle\langle\psi_i|$, with $|\psi_i\rangle$ being the eigenvectors, one can view the eigenvalue p_i as the (classical) probability that the system is in pure state $|\psi_i\rangle\langle\psi_i|$. In that sense the Von Neumann entropy is really exactly like the old classical entropy discussed earlier in equation (7), and the reader may find it helpful to view it as such.

Now it is clearly seen from equation (9) that for a pure state, in which $\rho = |\psi_i\rangle\langle\psi_i|$, the entropy is given by zero. The entropy arises whenever the state is mixed, and the eigenvalues of ρ are therefore different from strictly 1 and 0.

This paper will focus on calculating the entropy of subsystems and not of the total system however, which is trivially zero. When calculating the entanglement entropy of a subsystem A, one needs to insert the density operator ρ_A of that system in equation (8). To arrive at this density operator one takes the partial trace $\mathrm{Tr}\{\cdot\}$ over it's complement B in the total Hilbert Space $\mathcal{H}_{AB} = \mathcal{H}_A \otimes \mathcal{H}_B$. It is useful to show that this entropy $S_N(A)$ is equal to the entanglement entropy of the complementing subsystem $S_N(B)$, as the latter could be easier to calculate. Conceptually this is should be the case, since S_N is a measure for the entanglement of a subsystem with the rest of the environment. And since all the entanglement of A is with B, and vice versa, the entanglement that A has with the environment, B, should be equal to the entanglement that B has with the environment, A. This is easily shown mathematically using Schmidt decomposition. We can write the pure state $|\psi\rangle_{AB} = \sum_i \alpha_i |\chi_i\rangle \otimes |\xi_j\rangle \in \mathcal{H}_{AB}$, where $|\chi_i\rangle \in \mathcal{H}_A$ and $|\xi_j\rangle \in \mathcal{H}_B$. We have that $\rho_A = \mathrm{Tr}_B(|\psi\rangle\langle\psi|)$, and as seen before, this equals to $\rho_A = \sum_i |\alpha_i|^2 |\chi_i\rangle\langle\chi_i|$. It is clear that $|\alpha_i|^2$ are therefore the eigenvalues of ρ_A. A similar argument holds for the eigenvalues for ρ_B, which equal $|\alpha_i|^2$ as well. Since the entanglement entropy S_N can be calculated solely based on the eigenvalues, as seen in equation (9), it must mean that:

$$S_N(A) = S_N(B) \tag{13}$$

4.3 Area Law

It has been suggested from the principles of Black-Hole Thermodynamics that the entanglement entropy of an object in the groundstate scales with the size of its boundary [18], instead of it's volume like one might have expected. More specifically, a black-holes S_{BH} entropy is given by the Bekenstein-Hawking

equation: $S_{BH} = \frac{k_B A}{4l_p^2}$ [19]. This might be counter-intuitive, since one would imagine the number of particles to scale with the volume, and with it the information that can be stored. Let us bring the example of coins back. Think of a small box where 2 coins can fit in. Those coins are laid down randomly, a have a certain amount of possible configurations, namely $2^2 = 4$. The classical entropy will thus be $S = 2\ln 2$. If we would however have a box which has V times the volume, and could fit V times as many coins[5], the new entropy would be $S = 2V \ln 2$, resulting in volume scaling. Or that is what one could expect, but the reality for quantum particles is different. All that described the quantum coins in the box, and their information after their tossing is completely encrypted on the boundary.
To gain an intuition it is necessary to remember that the quantum entanglement entropy results from interaction between the different particles acted on by the Hamiltonian. Whenever a model is used to describe a quantum system, it is often assumed that the interactions of the particles are short-ranged. This seems to be in good correspondance with reality. The entanglement entropy is a measure of the correlation between two regions of space. If those regions interact merely due to short-ranged interactions, that interaction happens almost exclusively on the boundary of the regions. Since it seems intuitive that the correlation between two regions depends on the interaction between them, this correlation and thus the entanglement entropy scales with the boundary. This is beautifully illustrated in figure 2, which is an illustration taken from [20]. We will denote this area law as

$$S_N(A) \propto |\partial(A)| = aL^{d-1} \tag{14}$$

Where S_N is our usual Von-Neumann Entropy, A the subsystem whose entropy is measured and $\partial(A)$ its boundary. d is the spatial dimensionality of the system, L is the size of the system, and a a factor depending on the shape and dimension. For cubic shapes this factor is $a = 1$ in any dimension. Let us quickly also give the definition of the boundary $\partial(A)$.

Definition. (Boundary) Consider a set of lattice points Λ and a set of points forming the subsystem A. Let (a, b) be a neighbouring pair with $a \in A$ and $b \in \Lambda \setminus A$. The **boundary** $\partial(A)$ is the set of all such different neighbouring pairs.

Now this interaction has been studied for many years and on many different models: One dimensional and higher dimensional models, discrete and continuous space models, bosonic and fermionic systems. Several interesting results have come from this research, which this research will try to verify. This paper will focus on discrete fermionic models specifically.
Let us first discuss the one dimensional (fermionic) case, which has been studied very well in recent decades. It has been shown that, for critical systems, the entropy diverges logarithmically and otherwise it converges to a finite value [21, 22]. Further notes on critical systems will be given in the remainder of this chapter. The analytic derivation of the area-law for the 1 dimensional Ising model will be given in the next chapter. In higher dimensions it gets more interesting, as analytic models have not been found for the general case [20], although for non-critical bosonic systems analytic expressions are known [23]. What has been noticed however that the area-law seems be violated for critical models. In that case a logarithmic factor has been added to the relation, to insert lower and upper bounds for the entropy. As derived in [24], the violation is given by:

$$c_- L^{d-1} \ln L \leq S_N \leq c_+ L^{d-1} (\ln L)^2 \tag{15}$$

Here $c_\pm$ are constants determined by the Fermi-sea of the electrons. This has connections to conformal field theory, but is beyond the scope of this thesis. This violation of the area-law holds for cubic systems with side-length L. The factor $\ln(L)^2$, instead of just $\ln(L)$, in the upper bound is possibly an effect due to the lacking mathematical tools at our disposal for calculating the upper bounds, as noted in [25]. It has to be noted that for non-critical 1 dimensional models the area-law is known to hold, and interestingly enough also for bosonic critical models [26].

[5] Assuming perfect packing

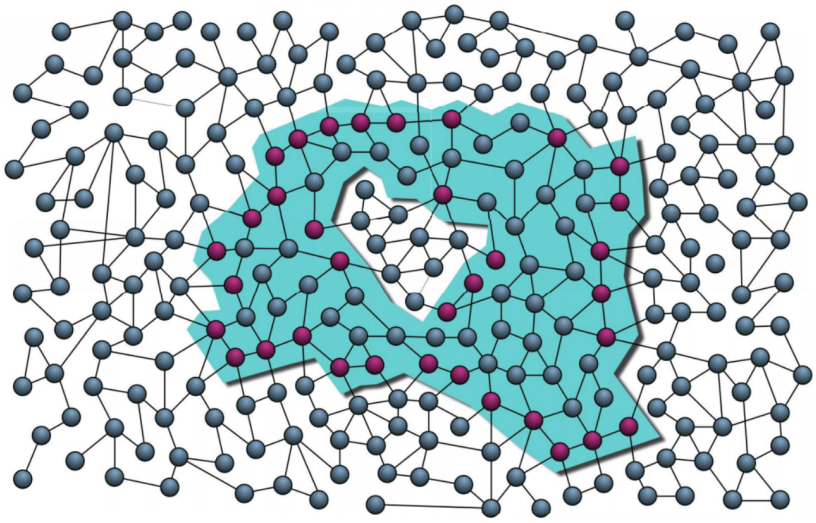

Figure 2: Illustration depicting the neighbouring interactions between particles. The shaded area A merely interacts with its complement through the dark-purple particles. If the correlation between the two regions only is due to the boundary, which we will learn happens if this correlation decays exponentially with distance, than the correlation scales with the size of the boundary $|\partial A|$. This illustration is taken from [20].

4.4 Correlation function

Now since there apparently (eq.14 vs eq.15) is a dissonance between critical and non-critical systems, it seems appropriate to provide with a clear distinction between them. Generally[6] speaking a system is critical whenever it is passed a point where it undergoes a phase-transition. At that point some quantity passes a critical value. This can be due to the increase of temperature, magnetic field strength, system size or some other variable. The phase-transition describes a change in qualitative behaviour of the system. Quantum spin systems that are studied in this paper are non-critical whenever the so-called 'connected correlation' or simply correlation decays exponentially with the distance between two sites. Inversely systems are called critical whenever the correlation does not decay exponentially. The correlation between i and j, for a certain operator O working on either site, is given by as

$$\langle O_i; O_j \rangle \equiv \langle \psi | O_i O_j | \psi \rangle_c \equiv \langle \psi | O_i O_j | \psi \rangle - \langle \psi | O_i | \psi \rangle \langle \psi | O_j | \psi \rangle \tag{16}$$

where $|\psi\rangle$ denote the statevector of a system. In our model, as will be apparent later, the operator used to calculate the correlation is the spin operator σ^z. This operator corresponds to the observable spin of the spin-$\frac{1}{2}$ fermions that will be studied in this thesis.
The area-law (14) thus seems to hold, whenever this notion of correlation decays exponentially with distance

$$\langle \sigma_i^z; \sigma_j^z \rangle \propto e^{-d(i,j)/\xi} \tag{17}$$

Here ξ is the so called correlation length and $d(\cdot, \cdot)$ is the distance between two sites and depends on the chosen metric, as one can find in [26, 27].
Whenever the correlation length does not decay as in equation (17), the critical region is reached and the area-law is expected to be violated up to the logarithmic correction in equation (15).

[6] vaguely

5 The Quantum Model

In this final section, that discusses the theory behind the paper, the used quantum mechanical models will be studied. We will apply the earlier knowledge to these models to simulate the quantum mechanical system in the thesis.
As stated before, this thesis will consider the behaviour of spin-$\frac{1}{2}$ fermions. These will be the particles discussed in the rest of this section and that will be simulated further in the thesis.

5.1 The Ising Model

The Ising model is a well studied model in solid state physics. It assumes that the Hamiltonian of the system solely consists of spin interaction between neighbouring particles and the coupling between each particle and the magnetic field. In this paper, the particles will be described in a lattice, either in 1 or 2 dimensions. The neighbouring particles will simply be those that are either one horizontal distance position away or one vertical distance away in the lattice, thus a distance of 1 in the L^1-norm: $d(i,j) = \|i-j\|_1 = 1$.
In the Ising model each site i in the lattice is given a discrete spin $\sigma_i \in \{-1, 1\}$. The total energy of the spin-configurations is given by the system Hamiltonian:

$$\hat{H} = -\sum_{\langle ij \rangle} J_{ij}\sigma_i\sigma_j + \lambda \sum_i B_i\sigma_i \tag{18}$$

Here J_{ij} gives the coupling between sites i and j, B_i gives the external magnetic field interaction at site i and λ is the standard magnetic moment of a particle.

This Hamiltonian can be rewritten into operator form, which will be useful for the simulation later. It shall be written as:

$$\hat{H}_{Ising} = -(\sum_{i,j} J^x_{ij}\sigma^x_i\sigma^x_j + J^y_{ij}\sigma^y_i\sigma^y_j + J^z_{ij}\sigma^z_i\sigma^z_j) + \lambda \sum_i B_i\sigma^z_i \tag{19}$$

Here σ^γ_i is the Pauli matrix σ^γ working on particle i. The Pauli matrices deal with the particle spins and are defined as:

$$\sigma^x = \begin{pmatrix} 0 & 1 \\ 1 & 0 \end{pmatrix} \qquad \sigma^y = \begin{pmatrix} 0 & -i \\ i & 0 \end{pmatrix} \qquad \sigma^z = \begin{pmatrix} 1 & 0 \\ 0 & -1 \end{pmatrix} \tag{20}$$

5.2 The XY-model with periodic boundary conditions

For the model in this paper some simplifying assumptions are made. It is assumed that $J^z_{ij} = 0$. Following [26] we define $J^x_{ij} = \frac{1+\gamma}{2}$ and $J^y_{ij} = \frac{1-\gamma}{2}$ to form the XY-model. The magnetic field interacts linearly with the field strength. For that $B_i = \frac{1}{2}$ is taken to perserve symmetry. The resulting Hamiltonian (19) can be rewritten as:

$$\hat{H}_{XY} = -\sum_{\langle ij \rangle} (\frac{1+\gamma}{2}\sigma^x_i\sigma^x_j + \frac{1-\gamma}{2}\sigma^y_i\sigma^y_j) + \frac{\lambda}{2}\sum_i \sigma^z_i \tag{21}$$

Where γ is responsible for prefered assymetry. If $\gamma = 0$ one retrieves the so-called XX-model.

in order to perform numerical calculations, it would be necessary to have a finite number of particles in the system. This necessarily also leads to a boundary on the system with certain boundary conditions. It is common [20, 26] to impose periodic boundary conditions by identifying opposite boundaries parallel-wise. Depending on the dimension of the system this basically means one forms a

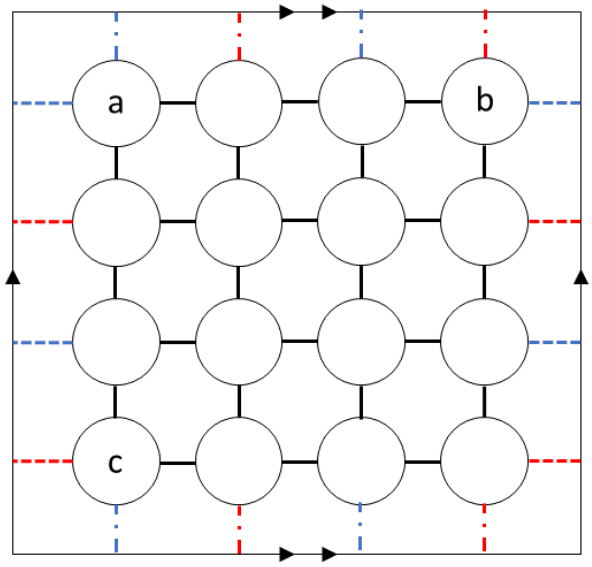

Figure 3: Example of a 4×4 lattice with periodic boundary conditions. The arrows on the boundary indicates that the upper boundary is identified with the bottom, similar for the left and right boundary. This leads to the fact that the neighbouring interactions happen 'through' the boundary. The corresponding blue and red colors, together with the line-type, are used to clarify which particles interact. Particle a, for example, interacts with particles b and c, next to its right and bottom neighbours

space topologically isomorphic to a torus. More specifically, for dimension d and a lattice Λ with N_i gridpoints in direction i, the formed space is equivalent to:

$$\Lambda = \bigotimes_{i=1}^{d} \mathbb{Z}/(N_i\mathbb{Z}) \tag{22}$$

Or equivalently the states have the property:

$$\forall p_i \in \mathbb{Z} : |\psi(p_1, p_2, \ldots, p_i, \ldots, p_{d-1}, p_d)\rangle = |\psi(p_1, p_2, \ldots, p_i + N_i, \ldots, p_{d-1}, p_d)\rangle \tag{23}$$

Where $|\psi(\vec{r})\rangle$ gives the representation of $|\psi\rangle$ in the discrete space. Due to the boundary condition (23), there is some obvious induced translational symmetry, and it gives us the ability to analyse the system in a numeric fashion. It should be noted by the reader that this means that for a 2D-lattice with sidelengths of N points, the gridpoints at position $(1, 1)$ and $(N, 1)$ are neighbouring and thus interact. This is visualised in figure 3.

5.3 1 Dimensional model and Entanglement Entropy

Consider the XX-model Hamiltonian in which equation (21) has $\gamma = 0$ and the boundary condition (22) in one dimension and N particles:

$$\hat{H}_{XX} = -\frac{1}{2}\sum_{i=0}^{N-1}(\sigma_i^x\sigma_{i+1}^x + \sigma_i^y\sigma_{i+1}^y) + \frac{\lambda}{2}\sum_{i=0}^{N-1}\sigma_i^z \tag{24}$$

We will solve the ground state of system (24) analytically. Thereafter it is possible to derive an expression of the entanglement entropy for a subsystem as a function of the subsystem length. The approach used for this derivation is taken from [26]. This 1D approach will be used as a template to apply to the 2D case in order to find an analytic expression. It will be clear that this approach will not work in this 2 dimensional problem however.

5.3.1 Ground State

To compute the groundstate, needed for calculating the entanglement entropy, we will start by performing a Jordan-Wigner transform. With it the Hamiltonian $\hat{H}_{XX}$ is written in terms of fermionic creation and annihilation operators, after which a Fourier transform is applied and the groundstate can be produced. If one would be dealing with the XY-model (21), then it would also be necessary to perform so-called 'Bogoliubov' transforms, but this is not necessary. This computation is standard and also outlined in [28–30]. We will however follow [26] and provide additional steps ourselves.

Starting with the Jordan-Wigner transform, we the fermionic creation $a_l^\dagger$ and annihilation a_l operators at site l as are defined with use of the Pauli-matrices (20) as:

$$a_l = \prod_{k=0}^{l-1}(\sigma_k^z)\frac{\sigma_l^x - i\sigma_l^y}{2} \qquad \text{and} \qquad a_l^\dagger = \left(\frac{\sigma_l^x - i\sigma_l^y}{2}\right)^\dagger \prod_{k=0}^{l-1}(\sigma_k^z)^\dagger \tag{25}$$

Note that these are each others unique conjugation in the C*-algebra. These operators follow the usual fermionic anticommutation relations (3). It is useful to realise that:

$$\frac{\sigma_m^x - i\sigma_m^y}{2} = \begin{pmatrix} 0 & 0 \\ 1 & 0 \end{pmatrix}_m \tag{26}$$

It is instructive to show that the anticommutation relations indeed hold for the operators in (25). For this derivation it is important to note that the spin-operators working on different sites commute: $\sigma_i^\gamma \sigma_j^\delta = \sigma_j^\delta \sigma_i^\gamma$ for $i \neq j$. Let's proof the first relation. First assume that $m < l$, afterwords the case of $m = l$ will be covered, with no loss of generality.

$$\begin{aligned}\{a_l, a_m\} &= a_l a_m + a_m a_l \\ &= \prod_{k=0}^{l-1}(\sigma_k^z)\frac{\sigma_l^x - i\sigma_l^y}{2}\prod_{\tilde{k}=0}^{m-1}(\sigma_{\tilde{k}}^z)\frac{\sigma_m^x - i\sigma_m^y}{2} + \prod_{k=0}^{m-1}(\sigma_k^z)\frac{\sigma_m^x - i\sigma_m^y}{2}\prod_{\tilde{k}=0}^{l-1}(\sigma_{\tilde{k}}^z)\frac{\sigma_l^x - i\sigma_l^y}{2}\end{aligned} \tag{27}$$

Since $m \in \{1, 2, \ldots, l-2, l-1\}$ and therefore expression (26) anti-commutes with σ_m^z, we get:

$$\begin{aligned}\{a_l, a_m\} &= \prod_{k=0}^{l-1}(\sigma_k^z)\prod_{\tilde{k}=0}^{m-1}(\sigma_{\tilde{k}}^z)\frac{\sigma_l^x - i\sigma_l^y}{2}\frac{\sigma_m^x - i\sigma_m^y}{2} - \prod_{k=0}^{m-1}(\sigma_k^z)\prod_{\tilde{k}=0}^{l-1}(\sigma_{\tilde{k}}^z)\frac{\sigma_m^x - i\sigma_m^y}{2}\frac{\sigma_l^x - i\sigma_l^y}{2} \\ &= 0\end{aligned} \tag{28}$$

To get to the last equality, we've used that spin-operators at different sites commute, and obviously σ_k^z commutes with itself, to form the last equality.
Now for $l = m$ we have have that:

$$\begin{aligned}\{a_l, a_l\} &= 2a_l a_l \\ &= 2\prod_{k=0}^{l-1}(\sigma_k^z)\frac{\sigma_l^x - i\sigma_l^y}{2}\prod_{\tilde{k}=0}^{l-1}(\sigma_{\tilde{k}}^z)\frac{\sigma_l^x - i\sigma_l^y}{2} \\ &= 2(\prod_{k=0}^{l-1}(\sigma_k^z)\frac{\sigma_l^x - i\sigma_l^y}{2}\frac{\sigma_l^x - i\sigma_l^y}{2}\prod_{k=0}^{l-1}(\sigma_k^z)) \\ &= 2\prod_{k=0}^{l-1}(\sigma_k^z)\cdot 0 \cdot \prod_{k=0}^{l-1}(\sigma_k^z) = 0\end{aligned}$$

Which holds since by filling in equation (26). The same derivation holds for the relation $\{a_l^\dagger, a_m^\dagger\} = 0$ by taking the conjugate transpose in the C^*-algebra at each step. With this the first relation in (3) is proven. Now the second relation $\{a_l^\dagger, a_m\} = \delta_{ij}$ will be proven. Again by first assuming $m < l$:

$$\begin{aligned}
\{a_l^\dagger, a_m\} &= \prod_{k=0}^{l-1} \left(\frac{\sigma_l^x - i\sigma_l^y}{2}\right)^\dagger (\sigma_k^z)^\dagger \prod_{k=0}^{m-1} (\sigma_k^z) \frac{\sigma_m^x - i\sigma_m^y}{2} + \prod_{k=0}^{m-1} (\sigma_k^z) \frac{\sigma_m^x - i\sigma_m^y}{2} \prod_{k=0}^{l-1} \left(\frac{\sigma_l^x - i\sigma_l^y}{2}\right)^\dagger (\sigma_k^z)^\dagger \\
&= \prod_{k=0}^{l-1} (\sigma_k^z)^\dagger \prod_{k=0}^{m-1} (\sigma_k^z) \left(\frac{\sigma_l^x - i\sigma_l^y}{2}\right)^\dagger \frac{\sigma_m^x - i\sigma_m^y}{2} - \prod_{k=0}^{m-1} (\sigma_k^z) \prod_{k=0}^{l-1} (\sigma_k^z)^\dagger \frac{\sigma_m^x - i\sigma_m^y}{2} \left(\frac{\sigma_l^x - i\sigma_l^y}{2}\right)^\dagger \\
&= 0
\end{aligned}$$

Where similar reasoning as in (27,28) is used. Finally for $m = l$:

$$\begin{aligned}
\{a_l^\dagger, a_l\} &= \prod_{k=0}^{l-1} \left(\frac{\sigma_l^x - i\sigma_l^y}{2}\right)^\dagger (\sigma_k^z)^\dagger \prod_{k=0}^{l-1} (\sigma_k^z) \frac{\sigma_l^x - i\sigma_l^y}{2} + \prod_{k=0}^{l-1} (\sigma_k^z) \frac{\sigma_l^x - i\sigma_l^y}{2} \prod_{k=0}^{l-1} \left(\frac{\sigma_l^x - i\sigma_l^y}{2}\right)^\dagger (\sigma_k^z)^\dagger \\
&= \prod_{k=0}^{l-1} (\sigma_k^z)^\dagger \prod_{k=0}^{l-1} (\sigma_k^z) \left(\frac{\sigma_l^x - i\sigma_l^y}{2}\right)^\dagger \frac{\sigma_l^x - i\sigma_l^y}{2} + \prod_{k=0}^{l-1} (\sigma_k^z) \prod_{k=0}^{l-1} (\sigma_k^z)^\dagger \frac{\sigma_l^x - i\sigma_l^y}{2} \left(\frac{\sigma_l^x - i\sigma_l^y}{2}\right)^\dagger
\end{aligned}$$

So far we've only done some trivial commuting. Now note that $(\sigma_k^z)^\dagger = \sigma_k^z$, and that $(\sigma_k^z)^2 = \mathbb{1}$. :

$$\begin{aligned}
\{a_l^\dagger, a_l\} &= \prod_{k=0}^{l-1} (\sigma_k^z)^2 \left(\frac{\sigma_l^x - i\sigma_l^y}{2}\right)^\dagger \frac{\sigma_l^x - i\sigma_l^y}{2} + \prod_{k=0}^{l-1} (\sigma_k^z)^2 \frac{\sigma_l^x - i\sigma_l^y}{2} \left(\frac{\sigma_l^x - i\sigma_l^y}{2}\right)^\dagger \\
&= \left(\frac{\sigma_l^x - i\sigma_l^y}{2}\right)^\dagger \frac{\sigma_l^x - i\sigma_l^y}{2} + \frac{\sigma_l^x - i\sigma_l^y}{2} \left(\frac{\sigma_l^x - i\sigma_l^y}{2}\right)^\dagger = \mathbb{1}
\end{aligned}$$

For the final equality equation (26) is simply applied.
Now that it is clear that this transform indeed produces the annihilation and creation operators with the desired fermionic anti-commutation relations (3) we can proceed to actually perform this transform, following the steps outlined in [26].

Rewriting $\hat{H}_{XX}$ (again from equation (24)) for a total number of N particles after preforming the Jordan-Wigner transform:

$$\hat{H}_{XX} = -\sum_{l=0}^{N-1} \left(a_l^\dagger a_{l+1} + a_{l+1}^\dagger a_l\right) + \lambda \sum_{l=0}^{N-1} a_l^\dagger a_l \tag{29}$$

This can also be recognised as a free fermion model with chemical potential λ. We let $\lambda \geq 0$, otherwise we can reassign the z-axis direction of the system, by interchanging what is considered up and down, without loss of generality. For example if $\lambda < 0$, then by interchanging the spin direction the lowering a_l operator would become the raising operator $\tilde{a}_l^\dagger$ and vice versa. This are good fermionic operators by relations (3). The equivalent of Hamiltonian (29) will become:

$$\begin{aligned}
\tilde{H}_{XX} &= -\sum_{l=0}^{N-1} \left(-\tilde{a}_l^\dagger \tilde{a}_{l+1} - \tilde{a}_{l+1}^\dagger \tilde{a}_l\right) + \lambda \sum_{l=0}^{N-1} (1 - \tilde{a}_l^\dagger \tilde{a}_l) \\
&= \sum_{l=0}^{N-1} \left(\tilde{a}_l^\dagger \tilde{a}_{l+1} + \tilde{a}_{l+1}^\dagger \tilde{a}_l\right) - \lambda \sum_{l=0}^{N-1} (\tilde{a}_l^\dagger \tilde{a}_l) + \lambda(N-1)
\end{aligned} \tag{30}$$

This clearly is a bijective transformation, and we can therefore assume that $\lambda \geq 0$, since otherwise we can equivalently consider this transform with the flipped sign.
Now the Hamiltonian (29) can be Fourier transformed by introducing the transform for the fermionic operators:

$$b_k = \frac{1}{\sqrt{N}} \sum_{l=0}^{N-1} a_l e^{-2\pi i k l/N} \tag{31}$$

where $0 \leq k \leq N-1$. The $b_k^\dagger$ operator is just the conjugate of b_k. These also satisfy the standard anti-commutation relations (3) and are therefore fermionic operators, since the Fourier transform is a unitary operation.
The resulting Hamiltonian now written with these new Fourier Transformed operators is diagonizable:

$$\hat{H}_{XX} = \sum_{k=0}^{N-1} \Lambda_k b_k^\dagger b_k \tag{32}$$

where we take:

$$\Lambda_k = \lambda - 2\cos\frac{2\pi k}{N} \tag{33}$$

This diagonalised form is possible since the periodic boundary condition work neatly with the Fourier transform.
It is instructive to derive this diagonalisation. In order to do so, one needs to use the well-known equation:

$$\sum_{m=0}^{M-1} e^{2\pi i (n-\tilde{n}) m/M} = M\delta_{n\tilde{n}} \tag{34}$$

This firstly can be used to derive the inverse Fourier Transform

$$a_l = \frac{1}{\sqrt{N}} \sum_{k=0}^{N-1} b_k e^{2\pi i k l/N} \tag{35}$$

Using this reverse transform, we can substitute a_l and its conjugate $a_l^\dagger$ in the given Hamiltonian (29):

$$\begin{aligned}
\hat{H}_{XX} =& -\sum_{l=0}^{N-1} \Bigg(\left[\frac{1}{\sqrt{N}} \sum_{k=0}^{N-1} b_k^\dagger e^{-2\pi i k l/N}\right] \left[\frac{1}{\sqrt{N}} \sum_{\tilde{k}=0}^{N-1} b_{\tilde{k}} e^{2\pi i \tilde{k}(l+1)/N}\right] \\
&+ \left[\frac{1}{\sqrt{N}} \sum_{k=0}^{N-1} b_k^\dagger e^{-2\pi i k(l+1)/N}\right] \left[\frac{1}{\sqrt{N}} \sum_{\tilde{k}=0}^{N-1} b_{\tilde{k}} e^{2\pi i \tilde{k} l/N}\right] \Bigg) \\
&+ \lambda \sum_{l=0}^{N-1} \left(\left[\frac{1}{\sqrt{N}} \sum_{k=0}^{N-1} b_k^\dagger e^{-2\pi i k l/N}\right] \left[\frac{1}{\sqrt{N}} \sum_{\tilde{k}=0}^{N-1} b_{\tilde{k}} e^{2\pi i \tilde{k} l/N}\right] \right) \\
=& -\frac{1}{N} \sum_{l=0}^{N-1} \Bigg(\left[\sum_{k=0}^{N-1} \sum_{\tilde{k}=0}^{N-1} b_k^\dagger b_{\tilde{k}} e^{2\pi i(\tilde{k}-k) l/N} e^{2\pi i \tilde{k}/N}\right] \\
&+ \left[\sum_{k=0}^{N-1} \sum_{\tilde{k}=0}^{N-1} b_k^\dagger b_{\tilde{k}} e^{2\pi(\tilde{k}-k) l/N} e^{-2\pi i k/N}\right] \Bigg) \\
&+ \frac{\lambda}{N} \sum_{l=0}^{N-1} \left(\sum_{k=0}^{N-1} \sum_{\tilde{k}=0}^{N-1} b_k^\dagger b_{\tilde{k}} e^{2\pi i(\tilde{k}-k) l/N} \right)
\end{aligned} \tag{36}$$

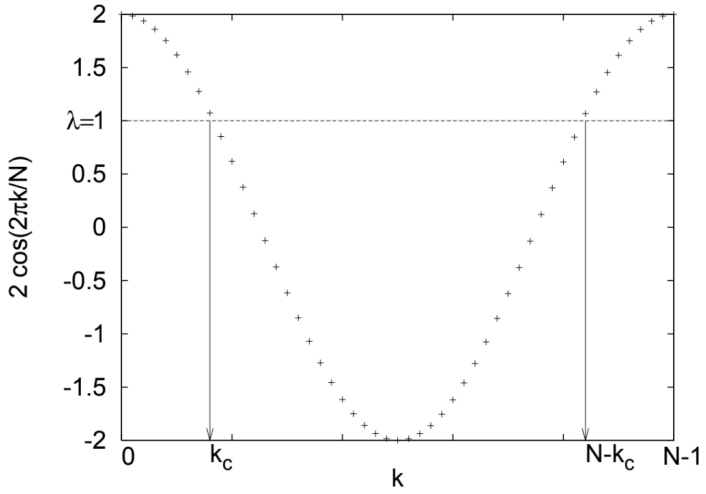

Figure 4: The plot displays the two terms of Λ_k as a function of k for $\lambda = 1$. It is clear that if $2\cos\frac{2\pi k}{N} > \lambda$, we have that $\Lambda < 0$ and if $2\cos\frac{2\pi k}{N} < \lambda$ we have $\Lambda > 0$. This plot is taken from [26].

When applying expression (35) to the final right-hand side of (36), specifically summing over l, one retrieves:

$$\begin{aligned}\hat{H}_{XX} &= -\left[\sum_{k=0}^{N-1}\sum_{\tilde{k}=0}^{N-1} b_k^\dagger b_{\tilde{k}} e^{2\pi i\tilde{k}/N}\delta_{k\tilde{k}}\right] - \left[\sum_{k=0}^{N-1}\sum_{\tilde{k}=0}^{N-1} b_k^\dagger b_{\tilde{k}}^{-2\pi ik/N}\delta_{k\tilde{k}}\right] + \lambda\left(\sum_{k=0}^{N-1}\sum_{\tilde{k}=0}^{N-1} b_k^\dagger b_{\tilde{k}}\delta_{k\tilde{k}}\right) \\ &= -\sum_{k=0}^{N-1}\left(b_k^\dagger b_k e^{2\pi ik/N} - b_k^\dagger b_k e^{-2\pi ik/N}\right) + \lambda\sum_{k=0}^{N-1} b_k^\dagger b_k\end{aligned} \tag{37}$$

Using the definition of the cosine and factoring out a few trivial terms, we readily can rewrite (37) into the desired form (32), concluding our proof.

Let us determine the properties of the ground state. It is clear by the properties of the ladder-operators, that for all vectors $|\psi\rangle$ we have:

$$0 \leq \left\| b_k^\dagger b_k |\psi\rangle \right\| \leq ||\psi\rangle| \tag{38}$$

Moreover, vectors which are eigenvectors for all $b_k^\dagger b_k$ will also be eigenvectors of $\hat{H}_{XX}$. Suppose we find a state $|GS\rangle$ such that whenever $\Lambda_k > 0$ we have $b_k^\dagger b_k |GS\rangle = 0$ and whenever $\Lambda_k < 0$ we have $b_k^\dagger b_k |GS\rangle = |GS\rangle$. In that case $|GS\rangle$ is an eigenvector of the Hamiltonian and also must have the lowest eigenvalue by 38, it therefore has to be the groundstate. In these cases it must be respectively that $b_k |GS\rangle = 0$ and $b_k^\dagger |GS\rangle = 0$. So the condition we the ground state needs to abide is:

$$\begin{aligned} b_k |GS\rangle &= 0 \text{ if } \Lambda_k > 0 \\ b_k^\dagger |GS\rangle &= 0 \text{ if } \Lambda_k < 0 \end{aligned} \tag{39}$$

Moreover the eigenvalue of this groundstate is given as $E_{GS} = \sum_{k|\Lambda_k<0} \Lambda_k$. The criterium of $\Lambda_k < 0$ is displayed in figure 4, where the two parts of Λ_k are displayed as a function of k. For $2\cos\frac{2\pi k}{N} > \lambda$, we have that $\Lambda < 0$.

5.3.2 Entanglement Entropy

In order to demonstrate the area-law we would like to compute the entanglement entropy of a block of L particles. Continuing to follow the approach written down by [26], we compute the correlation matrix

$\langle a_m^\dagger a_n \rangle$ of the ground state $|GS\rangle$. The coefficients of this matrix are calculated as $\langle GS| a_m^\dagger a_n |GS\rangle$. The eigenvalues of this matrix can be related to the eigenvalues of the reduced density matrix ρ_L. The coefficients the n, m are in this corresponding to particles inside the block L. These latter eigenvalues are necessary to compute the Von Neumann entropy as given by (9).
It is easy to compute the correlation matrix of the Fourier transform using the conditions (39):

$$\langle b_k^\dagger b_l \rangle \begin{cases} \delta_{kl} & \Lambda_k < 0 \\ 0 & \Lambda_k > 0 \end{cases} \tag{40}$$

In order to prove this, let us first consider $\langle b_k^\dagger b_l \rangle$ for $k \neq l$. Then b_l will annihilate any Fourier 'down' state $|-\rangle$ in index l and turn a 'up' $|+\rangle$ state into a down state. This newly created down state will obviously be orthogonal to the up state before the annihilation. So indeed $\langle b_k^\dagger b_l \rangle = \langle + |_l \, b_k^\dagger b_l \, |+\rangle_l = 0$. Now for $k = l$, we have that $b_k^\dagger b_k |GS\rangle = 0$ for $\Lambda_k > 0$ due to equation (39). For $\Lambda_k < 0$ we have that $b_k^\dagger b_k = \mathbb{1}$. All together this produces (40).
It is apparent that for $\lambda > 2$ we have that $\forall k : \Lambda_k > 0$ and thus $\forall k, l : \langle b_k^\dagger b_l \rangle = 0$ meaning that the correlation matrix $\langle a_m^\dagger a_n \rangle = 0$ and thus there are no correlations and $|GS\rangle$ is a product state. This case is therefore trivial, as there is no entanglement and therefore no entanglement entropy. We will therefore assume that $0 \leq \lambda \leq 2$.
It is now necessary to define some critical k_c for which it is true that $\Lambda_k \geq 0$ whenever $0 \leq k \leq k_c$ and $N - k_c \leq k \leq N - 1$. Looking at our definition (33) of Λ_k it must be that:

$$k_c = \lfloor \frac{N}{2\pi} \arccos \frac{\lambda}{2} \rfloor \tag{41}$$

where $\lfloor (\cdot) \rfloor$ is the floor function, just as described in [26]. Having introduced this, together with the known Fourier transform and the derived expression (40) we can derive the result that is provided in [26][7]:

$$\begin{aligned} \langle a_m^\dagger a_n \rangle &= \left\langle \frac{1}{\sqrt{N}} \sum_{k=0}^{N-1} b_k^\dagger e^{-2\pi i k m/N} \frac{1}{\sqrt{N}} \sum_{l=0}^{N-1} b_l e^{2\pi i l n/N} \right\rangle \\ &= \frac{1}{N} \left\langle \sum_{k=0}^{N-1} \sum_{l=0}^{N-1} b_k^\dagger b_l e^{-2\pi i k m/N} e^{2\pi i l n/N} \right\rangle \end{aligned} \tag{42}$$

Using (40) and the our new definition for k_c (41):

$$\begin{aligned} \langle a_m^\dagger a_n \rangle &= \frac{1}{N} \left(\sum_{k=0}^{k_c} e^{2\pi i k(n-m)/N} + \sum_{k=N-k_c}^{N-1} e^{2\pi i k(n-m)/N} \right) \\ &= \frac{1}{N} \left(\sum_{k=0}^{k_c} e^{2\pi i k(n-m)/N} + \sum_{k=-k_c}^{-1} e^{2\pi i k(n-m)/N + 2\pi i (n-m)} \right) \\ &= \frac{1}{N} \left(\sum_{k=0}^{k_c} e^{2\pi i k(n-m)/N} + \sum_{k=1}^{k_c} e^{-2\pi i k(n-m)/N} \right) \\ &= \frac{2}{N} \sum_{k=0}^{k_c} \cos\left(\frac{2\pi}{N} k(m-n) \right) - \frac{1}{N} \end{aligned} \tag{43}$$

In the final equality the exponential definition of the cosine is used.
In the thermodynamic limit where $N \to \infty$ this sum becomes an integral. One should be careful with

[7] We actually see that this is NOT the result from [26], since the factor $\frac{1}{N}$ is erroneously omitted there. It does not matter in the thermodynamic limit however

the limits of integration since k_c also goes to infinity. The resulting correlation matrix in this limit becomes.

$$A_{mn} \equiv \left\langle a_m^\dagger a_n \right\rangle = \frac{1}{\pi} \frac{\sin((k_c(m-n))}{m-n} \tag{44}$$

It should be noted that by Wick's theorem [31] any operator that acts on the block can be written in terms of the correlation matrix. This is true for this system since Gaussian systems like these are defined by their first and second moments, which is necessary for Wick's theorem to hold.
Still following [26], the correlation matrix of a block with size L can also be computed in another way to compute $\langle GS| a_m a_n |GS\rangle$. Since n and m are part of the block of the density matrix L:

$$A_{mn} = \mathrm{Tr}\{a_m a_n \rho_L\} \tag{45}$$

This is simply how to compute the expectation value using the density matrix by [32].
Now continuing the approach in the [26], it is needed to compute the density matrix ρ_L from relation (45) by what we know of A_{mn} form (44). A_{mn} can be diagonalized since it is Hermitian, and thus there is a diagonal matrix with entries G_{pq} and a unitary matrix with entries u_{rs} such that

$$G_{pq} = \sum_{n=0}^{N-1} \sum_{m=0}^{N-1} u_{pm} A_{mn} u_{nq}^* \tag{46}$$

The entries on its diagonal thus become $g_p = \sum_{m=0} u_{pm} a_m$. Since G_m is diagonal, and due to the definition of expectation value:

$$G_{mn} = \mathrm{Tr}\left\{g_m^\dagger g_n \rho_L\right\} = \nu_m \delta_{mn} \tag{47}$$

This means that ρ_L is uncorrelated and can be written as a product state

$$\rho_L = \varrho_1 \otimes \cdots \otimes \varrho_L \tag{48}$$

where ϱ_m is the density matrix corresponding to the m-th fermionic mode with the creation operator $g_m^\dagger$.
The eigenvalues can be determined whenever these operators are written in a matrix-representation. We shall define for some basis:

$$g_m = \begin{pmatrix} 0 & 1 \\ 0 & 0 \end{pmatrix}_m \qquad g_m^\dagger = \begin{pmatrix} 0 & 0 \\ 1 & 0 \end{pmatrix}_m \qquad \varrho_m = \begin{pmatrix} \alpha_m & \beta_m \\ \beta_m^* & 1-\alpha_m \end{pmatrix}_m \tag{49}$$

where we used some useful representation for the fermionic operators and the fact that the density operator is Hermitian with unit trace. Note that $0 \leq \alpha_m \leq 1 \in \mathbb{R}$. By symmetry and separation of product spaces, since we have that $\mathrm{Tr}\left\{g_n^\dagger g_m \rho_L\right\} = 0$ for any $m \neq n$ by equation (47), it must be for any m that $\mathrm{Tr}\{g_m \rho_L\} = 0$, and thus:

$$\mathrm{Tr}\{g_m \rho_L\} = \beta_m = 0 \tag{50}$$

Now using equation (47) again it is clear that

$$\nu_m = \mathrm{Tr}\left\{g_m^\dagger g_m \rho_L\right\} = \mathrm{Tr}\left\{ \begin{pmatrix} 1 & 0 \\ 0 & 0 \end{pmatrix} \begin{pmatrix} \alpha_m & 0 \\ 0 & 1-\alpha \end{pmatrix} \right\} = \alpha_m \tag{51}$$

Hence it is clear that $\alpha_m = \nu_m$.

Now we would like to calculate the entanglement entropy. By [26] the entropy is given by:

$$S_L = \sum_{l=1}^{L} (-\nu_l \ln(\nu_l) - (1-\nu_l)\ln(1-\nu_l)) \tag{52}$$

We can deduce this solution rather easily from equation (8) by noticing that the complete density matrix ρ_L can me written as a product state of diagonal matrices. $\rho_L \ln(\rho_L)$ will also be a diagonal matrix, whose diagonal elements are just $\kappa_\mu \ln(\kappa_\mu)$ where κ_μ are the diagonal entries of the ρ_L. Now, these entries are all the possible unique products, such that each product contains either α_m or $1-\alpha_m$ for each m. Thus there are 2^L possible products. Let S_μ correspond to one of these 2^L sets of elements whose product equals κ_μ.
We will prove by induction. Let us consider all 2^{L-1} subset of these sets S'_μ containing α_1, with κ'_μ being the product by multiplying all elements in $S'_\mu \setminus \alpha_1$. The elements of $\rho_L \ln(\rho_L)$ resulting from this are thus of the form $(\alpha_1\kappa'_\mu)(\ln(\alpha_1) + \ln(\kappa'_\mu))$. Since trace is taken over all the elements, let us sum over all factors containing $\ln \alpha_1$. Then one has $\alpha_1 \sum_\mu \kappa\mu(\ln \alpha_1)$. Since for each element in this sum of this form $\alpha_1\alpha_2 R \ln(\alpha_1)$ for some R of possible products, there is exactly one element of the form $\alpha_1(1-\alpha_2)R\ln(\alpha_1)$ which sum to $\alpha_1 R \ln \alpha_1$. This process continues until $\alpha_1 \ln \alpha_1$ remains. By similar construction, one could take every unique element from each ϱ_m, and it is clear that that all that remains in the final trace will be. (52).
From this it is now possible to compute how entropy scales with the size of the block L. As outlined by [22] and from [33] one can deduce that the resulting scaling of the entanglement entropy for the case where $\lambda = 0$ is given as:

$$S_N(L) = \frac{1}{3}\ln(L) + a \tag{53}$$

where a is a constant deduced in [33] using conformal field theory. The exact derivation of this equation is beyond the scope of this paper. The important thing is that the correlation is logaritmic. This behaviour persists also when λ increases, although the entropy will decrease for all sizes L. Only when $\lambda = 2$ is reached will the entropy saturate and be bounded, which is why originally it was assumed that $\lambda < 2$.

It has to be observed that in one dimension the area-law is not upheld, since it is considered that in 1D the system is always in a critical state. The system seems to follow the relation given by (15), being exactly equal to the lower bound.

5.3.3 2D Variant

Now that we have found an analytic expression as in [26] for the 1D case, there is noting holding us back to try a similar approach ourselves for the higher dimensional case. It will be clear that this approach does not work however. Let us first rewrite the Hamiltonian (21) in 2 dimensions, again for $\gamma = 0$ and a prefactor to make calculations simpler without loss of generality. Starting with the general form, only refering to neighbours and not the lattice topology.

$$\hat{H}_{XX} = -\frac{1}{2}\sum_{\langle ij\rangle}\left(\sigma_i^x\sigma_j^x + \sigma_i^y\sigma_j^y\right) + \frac{\lambda}{2}\sum_i \sigma_i^z \tag{54}$$

Now in a 2D lattice with a toroidal topology, each fermion in the lattice has four neighbours, two in the same row and two in the same column. We will take the vertical direction to be denoted by k with a period of M and in the horizontal l with a period of L. One retrieves the Hamiltonian

$$\hat{H}_{XX} = -\frac{1}{2}\sum_{k=1}^{M}\sum_{l=1}^{N}\left(\sigma_{k,l}^x\sigma_{k+1,l}^x + \sigma_{k,l}^y\sigma_{k+1,l}^y + \sigma_{k,l}^x\sigma_{k,l+1}^x + \sigma_{k,l}^y\sigma_{k,l+1}^y - \lambda\sigma_{k,l}^z\right) \tag{55}$$

Let us repeat the Jordan-Wigner transform as before. The new annihilation and creation operators are defined as:

$$a_{k,l} = \prod_{m=0}^{k}\prod_{n=0}^{l}(\sigma_{m,n}^z)(1-\delta_{mk}\delta_{nl})\frac{\sigma_{k,l}^x - i\sigma_{k,l}^y}{2} \quad \text{and} \quad a_{k,l}^\dagger = \left(\frac{\sigma_{k,l}^x - i\sigma_{k,l}^y}{2}\right)^\dagger \prod_{m=0}^{k}\prod_{n=0}^{l}(\sigma_{m,n}^z)^\dagger(1-\delta_{mk}\delta_{nl}) \tag{56}$$

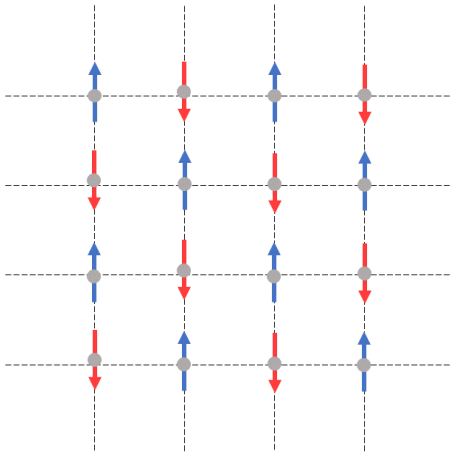

Figure 5: State of a 4×4 lattice with maximally misaligned spins. The spins alternate between being up and down. Another possible maximal misalignment state would be one in which all spins are flipped in comparison to this figure.

The Kronecker Delta δ_{pq} are introduced such that the only not present in the product would be the one in which $m = k$ and $n = l$. This is necessary such that the fermionic anti-commutation relations 3 are upheld. By performing this transform on the Hamiltonian (55) the following expression will be retrieved, by the same calculation as for the 1D case:

$$\hat{H}_{XX} = -\sum_{k=1}^{M}\sum_{l=1}^{N}(a_{k,l}^{\dagger}a_{k+1,l} + a_{k+1,l}^{\dagger}a_{k,l} + a_{k,l}^{\dagger}a_{k,l+1} + a_{k,l+1}^{\dagger}a_{k,l} - \lambda a_{k,l}^{\dagger}a_{k,l}) \tag{57}$$

Now a double Fourier transform can be taken in both the k and l direction. This transform defined analogously to 31 but with a double sum and a factor $\sqrt{MN}$ in the denominator. The results is the following formula:

$$\hat{H}_{XX} = \sum_{\mu=1}^{M}\sum_{\nu=1}^{N}\Lambda_{\mu\nu}b_{\mu,\nu}^{\dagger}b_{\mu,\nu} \tag{58}$$

Here $\Lambda_{\mu\nu} = \lambda - 2\cos\frac{2\pi\mu}{M} - 2\cos\frac{2\pi\nu}{N}$. Verifying this Hamiltonian in a numerical fashion, one will see that this is exactly our previous Hamiltonian we started with. In a similar manner as before we'd like to find the ground state. The complications start here however. By the previous course of action, we could easily define the eigenvalue of the groundstate, by summing the appropriate values for $\Lambda_{\mu\nu}$. Now this simply is not the case, as one can check numerically. One will see, that although there are indeed eigenvalues with the value $\sum_{\mu,\nu|\Lambda_{\mu,\nu}<0}\Lambda_{\mu,\nu}$, there are also eigenvalues lower than that. Therefore it will also not be of much use to continue searching for the eigenstates and the corresponding density operator.

Maybe it will be possible to simply guess the correct eigenstate of the system. Let us try guessing an eigenstate which should seem possible at first glance for the anti-ferromagnetic eigenstate of the crystal, where one could expect the spins all to be in maximal misalignment with their neighbours. An image of this ansatz can be seen in figure 5 for a 4×4 lattice. Notice however that the Hamiltonian

consist of a sum over all the neighbouring interactions, and the action on this neighbouring pair is such that their spins flip. It is clear that this happens when one considers that:

$$\frac{1}{2}(\sigma_i^x\sigma_j^x + \sigma_i^y\sigma_j^y) = \begin{pmatrix} & & & 0 \\ & & 1 & \\ & 1 & & \\ 0 & & & \end{pmatrix}_{i,j} \tag{59}$$

The maximally misaligned spins i, j are therefore exchanged, or flipped in other words. This means that, starting from our ansatz which is some basevector in the trivial spin-basis, the resulting vector after applying $\hat{H}_{XX}$ is a sum of strictly different basevectors. All of which are positive and different from the starting vector. A linear combination of the two possible misaligned ansatzes would not work either, since this will result in a linear combination of all these different basevectors which don't annihilate since they are still strictly different between each other. Therefore such a trivial solution for an eigenstate is not possible.

6 Numerical Model

The main part of this thesis concerns studying the relation between entropy and the area. Due to complications with the analytical approach, outlined in the previous section, this will be done numerically. This section will describe the computational model that was written to perform the numerical research. The first different part will focus on finding the eigenvectors of the system, specifically on the groundstate. For interest the spectrum of the system is also mapped. Continuing, the method to determine the subsystem and its entropy is described. Finally, it will be mentioned how the correlation of a system is calculated and how this is will be related to the possible existence of an area law. The actual code is written in MATLAB [34] and can be found in the Appendix. All code is run on computers with 8 RAM memory, either with 1 CPU or a 16 CPU cluster.

6.1 Eigenvectors, groundstate and spectrum

The first thing needed in order to analyse the area-law for entropy, is finding the groundstate for the Hamiltonian. The actual Hamiltonian for which the model has been written is given by:

$$\begin{aligned}\hat{H}_{Model} = -\sum_{i=1}^{M}\sum_{j=1}^{N}[&J_{i,j;i+1,j}\frac{1+\gamma}{2}\sigma^x_{i,j}\sigma^x_{i+1,j} + J_{i,j;i,j+1}\frac{1+\gamma}{2}\sigma^x_{i,j}\sigma^x_{i,j+1} \\ &+ J_{i,j;i+1,j}\frac{1-\gamma}{2}\sigma^y_{i,j}\sigma^y_{i+1,j} + J_{i,j;i,j+1}\frac{1-\gamma}{2}\sigma^y_{i,j}\sigma^y_{i,j+1}] + \frac{\lambda}{2}\sum_i\sum_j\sigma^z_{i,j}\end{aligned} \tag{60}$$

the Hamiltonian used in the model is a somewhat more generalized version of (21) for a 2D lattice, where the correlation could differ from one neighbouring pair to another. Also the pre-factor is slightly different from (21). This has no impact on the behaviour however, since that factor could be included in the correlation coefficients $J_{i,j;k,l}$. The exact value of $J_{i,j;k,l}$ does not matter, as one can scale this factor with any number, and have the same qualitative behaviour. What is important is the sign of $J_{i,j;k,l}$, as this can change the groundstate. Whenever the sign is positive, the systems is ferromagnetic. For negative signs, the system is anti-ferromagnetic. One also should keep in mind that the lattice is periodic, by (23). Therefore the site $(N+i,j)$ is equivalent to (i,j) for example.

6.1.1 Memory Limitations

We wish to calculate the eigenstates of $\hat{H}_{Model}$ (60), in particular the groundstate. There are numerous methods to compute eigenvalues and eigenvectors numerically, in the some of which are implemented in by default in MATLAB [34]. One can however quickly figure out that the provided methods are highly limited by computational memory.

Let us quickly calculate the required memory and how it scales with the system size. We know that the operators, like the Hamiltonian, can be represented by a matrix over the complex field. The dimensions of this matrix equals the dimension of the Hilbert space on which it acts. A particle-state of n spin-$\frac{1}{2}$ particles has a dimensionality of 2^n. Since each particle is described by a vector in the Hilbert space $\mathcal{H} = \mathbb{C}^2$. The combined system is therefore represented by vector in the Hilbert Space of n particles $\bigotimes_{i=0}^{n}\mathcal{H}_i = \mathbb{C}^{2\otimes n}$. One therefore needs $(2^n)^2 = 2^{2n}$ complex numbers to fully describe the Hamiltonian, or any operator, of such a system.

Let us assume that these numbers are stored that storing a number in the most basic form of the MATLAB float type `single`, which is a data-type constructed according to the IEEE Standard 754 for single precision numbers. This data-type uses 32 bits, and therefore 4 bytes. A complex number would, which is stored by two real (float) numbers, therefore needs 8 bytes of space. A single Hamiltonian for a system of $n = 16$ particles on a 4×4 grid, thus requires already 32 GB of RAM memory, to represent it as a full matrix. While this still is manageable, a 5×5 grid would already render the effort completely futile. A more practical way is needed to find the eigenvalues and -vectors of $\hat{H}$.

Since, in this specific case, the Hamiltonian $\hat{H}_{Model}$ mainly consists of zeros, it could be useful to introduce a so called sparse matrix. For this matrix, only the non-zero entries are saved, together with their indices. Constructing the sparse Hamiltonian representing equation (60) in a 4×4, approximately 66 MB of RAM space is required.
For our cause, it is more interesting to simulate even larger systems however. For 5×5 grids, even sparse matrices don't do the trick. They still requiring too much RAM memory for the computer this simulations are run on, which has a total of 8GB of RAM. From empirical research, the necessary memory of sparse matrices for $\hat{H}_{Model}$ is calculated to be given by $32(2^n + 2^{n+1}n + 1)$ bytes, where n is the amount of particles. For a 5×5 lattice this means the required memory is 51 Gigabytes. Now one approach could be to save the matrices on the Hard Disc and call them row by row. Note however that it would still be non-trivial to compute the eigenvalues if we would store the matrix in the hard memory, since we would not be able to perform operations on that matrix as a whole. Expanding the RAM memory would also be possible, but again, this scales terribly.

6.1.2 Hamiltonian as Operator

Another solution needs to be found, as a matrix representation seems unfeasible in any memory-wise. In stead of storing the Hamiltonian as a matrix, it is possible to construct the Hamiltonian as an operation working on vectors. The action of a single pair of spin-matrices on a vector are rather easily to compute. In order to compute the complete Hamiltonian, one just needs to compute these basic operations a multitude of times and sum the results, to retrieve $\hat{H}_{Model}$ 60. It will however not be trivial to determine the eigenvalues and vectors of the Hamiltonian, since we don't have a matrix, on which we could perform our linear algebra tricks. In order to compute these eigenvalues and -vectors another algorithm will be used, the so-called power method. The memory that is necessary for this computation merely scales with the $\mathcal{O}(n) = 2^n$ of the system as only the statevector needs to be stored (at most twice). This is an improvement over using the matrix-representation approach, the latter having $\mathcal{O}(n) = 2^{2n}$ memory-complexity.
Now the crux is to actually program the operator. That process consists of two main parts. The first part is determining all the neighbouring particles in the grid to perform the interaction on, which is done in a timely fashion by performing simple shifting operations on a template of a neighbouring pair, such that all the different pairs are covered. The details of this code are found in the Appendix A. Secondly it is needed to actually perform the actual interaction on the pairs of particles, after which the results can be summed over all the different neighbouring pairs. Since the $J_{i,j;k,l}$ in (60) is only pair dependent this is just prefactor of such a pair operation. The operation itself is due to the two x and y Pauli Matrices and which are weighted in terms of the γ variable. It is clear by the definition of the Pauli-matrices (20) that the terms in the sum of the $\hat{H}_{Model}$ are:

$$\frac{1+\gamma}{2}\sigma^x_{(i,j)}\sigma^x_{(k,l)} + \frac{1-\gamma}{2}\sigma^y_{(i,j)}\sigma^y_{(k,l)} = \begin{pmatrix} & & & \gamma \\ & & 1 & \\ & 1 & & \\ \gamma & & & \end{pmatrix}_{(i,j);(k,l)} \tag{61}$$

In our simulation we will basically use the fact that this operation on the two particles only requires 4 elementwise manipulations. The operation essentially multiplies each of the basevectors with either 1 or γ and inverts the up-down state of the two neighbouring particles. The multiplication can be done by elementwise multiplication with a vector with equal dimensionality to the original one the Hamiltonian acts on. This should fit in the memory, as the original vector does as well. These pairwise results need to be added together weighted by the correlation factor $J_{(i,j);(k,l)}$. Coding details are found in the Appendix.

6.1.3 Power Method

Now that we have found a way to memory-efficiently calculate the action of the Hamiltonian operator on some vector $|\psi\rangle$, it is key to design a method of determining the eigenvectors of this operator. The algorithm that will be used in this paper is the before-mentioned power method. This method specifically focuses on calculating the eigenvectors with the largest absolute eigenvalues. It consists of a simple iterative process. One starts with some random vector eigenvector $|\psi\rangle_0 \in \mathcal{H}$. At each step the algorithm performs the Hamiltonian operation on $|\psi\rangle_i$, after which $\hat{H}|\psi\rangle_{i+1}$ is normalized and the iteration is continued:

$$|\psi\rangle_{i+1} = \frac{\hat{H}_{Model}|\psi\rangle_i}{\left\|\hat{H}_{Model}|\psi\rangle_i\right\|} \tag{62}$$

where $|\psi\rangle_i$ is the random starting vector $|\psi\rangle_0$ after i iterations. The exact norm used does not make a difference theoretically. We shall see however that due to the large sizes of vectors numerical precision will play a large role and we shall be using the ∞-norm $\|\vec{v}\|_\infty = \max\{|v_1|, |v_2|, ...\}$. This is due to the fact that if a very large vector is normalized (of dimensionality 2^{25} for 5×5), the average entry will have significant digits in the order of 10^{-8}. This would come close to computational precision, and thus making the system error-prone.
It is necessary to see that the result of this process after many iterations is indeed the eigenvector with the absolute largest eigenvector. Indeed, when rewriting the statevector $|\psi\rangle$ vector in terms of eigenvectors one gets:

$$|\psi\rangle = \sum_{i=1}^{d} c_i |\phi_i\rangle \tag{63}$$

where d is the dimensionality of the system and c_i is the decomposition coefficients for eigenvector $|\phi_i\rangle$. Whenever the Hamiltonian acts on $|\psi\rangle$ one will have

$$\hat{H}_{Model}|\psi\rangle = \sum_{i=1}^{d} c_i E_i |\phi_i\rangle \tag{64}$$

where E_i is the corresponding eigenvalue. After renormalization, it is clear that the eigenvector with the largest $|E|$ will grow the most, and the one with smaller $|E_i|$ decrease relatively. Thus indeed, when the number of iterations i goes to infinity, $|\psi\rangle_i$ converges to the eigenvector of $\hat{H}$ whose eigenvalue is the absolute largest, given that it is not orthogonal to the random starting $|\psi\rangle_0$. This is true up to errors involving numerical precision, and some complications due to absolute values corresponding to multiple eigenvalues. We will tackle this complication now.
Our goal however is not to find the eigenvector with the absolute largest eigenvalue, but our goal is rather to find the groundstate. Supposing for example that there are multiple states with the largest absolute eigenvalue, which is either positive or negative since there are no complex eigenvalues for Hermitian operators. The resulting statevector after many iterations will be a linear combination of the eigenstates with those eigenvalues. In order to prevent finding large positive-eigenvalue states, it is possible to change the Hamiltonian used in the iteration a bit, by subtracting a scalar multiple of the unit-operation $a\mathbb{1}$ from it. Thus we take $\hat{H}_{iter} = \hat{H}_{Model} - a\mathbb{1}$. Since all vectors are eigenvectors of the unit operation, the eigenstates of $\hat{H}_{iter}$ will also be eigenstates of $\hat{H}_{Model}$, only with the eigenvalues be lowered by a. When a is larger than the eigenvalue of $\hat{H}_{Model}$, it is sure that the eigenvector corresponding to the original groundstate of $\hat{H}_{Model}$ will be also the eigenvector corresponding to the largest absolute eigenvector of $\hat{H}_{iter}$.

Let's quickly adress the problem when the random starting vector is orthogonal to the eigenvector corresponding to the groundstate. The probability of this happening is tiny. Normally[8] the probability would even be zero. After all, the orthogonal vectorspace is a plane of one dimension smaller than

[8] Read: Theoretically

the Hilbert Space, or more specifically on a unit-sphere intersecting that plane. The measure of such a sphere-plane intersection is zero in the original projective Hilbert Space (using standard Lebesgue measure) and thus the probability of a random numbers used to represent $|\psi\rangle_0$ landing on it should be zero. However, since the calculation is performed on a computer, numerical precision is at play.
In order to calculate the actual probability, lets introduce some necessary equations. Using the same template, the surface area of a unit-sphere in a d-dimensional Hilbert space and the circumference of the circle given by a plane intersecting that sphere is given respectively by:

$$S_{d-1} = \frac{2\pi^{\frac{d}{2}}}{\Gamma(\frac{d}{2})} \qquad \text{and} \qquad S_{d-2} = \frac{2\pi^{\frac{d-1}{2}}}{\Gamma(\frac{d-1}{2})} \tag{65}$$

Here $\Gamma(\cdot)$ is the Gamma function. The probability $\mathbb{P}_\perp$ of a random vector being in the orthogonal strip to some other vector is approximately

$$\mathbb{P}_\perp = \frac{S_{d-2}\epsilon}{S_{d-1}} = \frac{\pi^{-\frac{1}{2}}\Gamma(\frac{d-1}{2})\epsilon}{\Gamma(\frac{d}{2})} \tag{66}$$

Here ϵ indicates numerical precision. This value can be simplified using the formula:

$$\Gamma(\frac{n}{2}) = \sqrt{\pi}\frac{(n-2)!!}{2^{\frac{n-1}{2}}} \tag{67}$$

where the canonical definition of the double factorial is used. Combining (66) and (67):

$$\mathbb{P}_\perp = \frac{\sqrt{2}(d-3)!!\epsilon}{\sqrt{\pi}(d-2)!!} \tag{68}$$

It is trivial by the definition of the double factorial that:

$$\frac{(d-3)!!}{(d-2)!!} = \prod_{i=k}^{d-3}\frac{i}{i+1} = \frac{k}{d-2} \tag{69}$$

Where $k = 2$ for even d and $k = 1$ for odd d. Due to the nature of the system, d is even. Thus by (69) and since $\sqrt{2/\pi} < 1$ we have that $\mathbb{P}_\perp < 2\epsilon/(d-2) < 10^{-8}$ for any of our systems, where we assumed numerical precision of $\epsilon \approx 10^{-8}$ and $d > 4$. Since for our all simulation, we use more than 4 particles at least, $d \geq 2^{16}$. This means the probability of a random vector being numerically orthogonal to our sought for eigenvector is infinitesimal. We therefore will assume that the random vector is not orthogonal to the groundstate, and the vector resulting from a perfect power method will indeed converge to the groundstate.

Having found the groundstate eigenvector, it is trivial to find the eigenvalue by performing another Hamiltonian operation on that eigenvector and determining the scaling factor by elementwise division. Every scaling factor should be exactly equal to the eigenvalue, whenever the vector really is the eigenvector of the operation. It could however happen that the resulting scaling factors are not all equal, because the vector is not really an eigenvector of the operation. This can for example occur if not enough iterations were taken in the process. The mean of the elements will be considered the estimate for the eigenvalue. The 'goodness' of the estimate is determined by the standard deviation of the values. By extension this also gives a measure of the 'goodness' of the found eigenstate.
This measure for 'goodness', using the standard deviation in the expected eigenvalue, is one of the stopping criteria for the algorithm. If after an iteration the standard deviation σ_i is less then $10^{-5} > \sigma_i$ the power method is aborted. Another criteria is whenever some number of iterations is reached, usually $T = 6000$. A final possible stopping criteria is when, up to numerical precision, there is no element-wise difference between two iterations of the power method.

It is also necessary to set very small values within the vector to zero, otherwise complications will arise. These include division by zero errors or the values being not exactly zero and leading to very inaccurate numbers after division, since numerical numbers lie on a discrete spectrum. Therefore after each iteration small numbers beneath a certain threshold are set to zero. It can be seen that the threshold has impact on the final standard deviation of the eigenvalues. This threshold can be changed depending on the problem, to try to find results with the lowest standard deivation. In general it seems that, when using the ∞-norm, a threshold of 10^{-5} gives nice results. This threshold will be therefore be used constantly in the paper. For programming details, one can refer to the code in the Appendix A.

6.1.4 Spectrum

To have a good understanding of the Hamiltonian and how its degeneracy changes when tweaking the different values for γ, λ and of course $J_{(i,j);(k,l)}$, it is necessary to obtain a good view of the spectrum of the Hamiltonian. The power method however only can be used to find the eigenvector with the absolute largest eigenvalue, and thus can at most be used to find the highest or lowest eigenvalue by the tricks mentioned before. An additional operation needs to be done, in order to find the other eigenvectors. After each iteration the components of $|\psi\rangle_i$ in the orthogonal complement to already found eigenvectros is calculated. This is essentially done by Gramm-Schmidt orthogonalisation. This makes sure that new eigenvectors are found, with possibly new eigenvalues. Whether these eigenvalues are new indeed, depends on the spectrum.

6.2 Subsystems and Entropy

Now that the different eigenstates, and more specifically the groundstate, are found it is time for the next step: Determining the entanglement entropy of a subsystem, and observing how it scales with the subsystems size.

6.2.1 Suitable Subsystems in periodic spaces

To determine the entanglement entropy of subsystems, it is first necessary to determine the subsystems themselves. The focus of this subsection will lie in actually deciding the subsystem-shape that will be chosen for the research.

The first choice that is made in this paper when deciding the shapes, is that the shapes are preferred to be convex. Convex and non-convex shapes tend to have a somewhat different relation in terms of their entropy-scaling, as has been pointed out in [35]. We will quickly introduce our own definition of convex and show how this produces complications in our toroidal topology. (22).

Definition. (Convex) Let A be a set of lattice points, and let P be the set of all shortest paths connected any two elements of A. We call A **convex** whenever all these shortest paths are subsets of A.

This is in line with the standard definition of convex, where a straight line connecting any two points of a shape must be completely inside that shape. The space is discrete however in our case, and we have to use this new definition, as straight lines are not always exist. Extra care should be taken to compare all the different shortest paths, since due to the discrete topology, not to mention due the toroidal nature of the topology, multiple shortest paths are possible, .

Now that the complications arising from the discreteness are covered, it remains to look at the additional complications due to the toroidal topology. Suppose the total system has sidelengths $N \times M$, i.e. the periodic boundary conditions have a period of N and M respectively. Within this system a rectanglular subsystem of sidelengths $(N-1) \times 1$ is picked, see figure 6. The rectangle is a shape

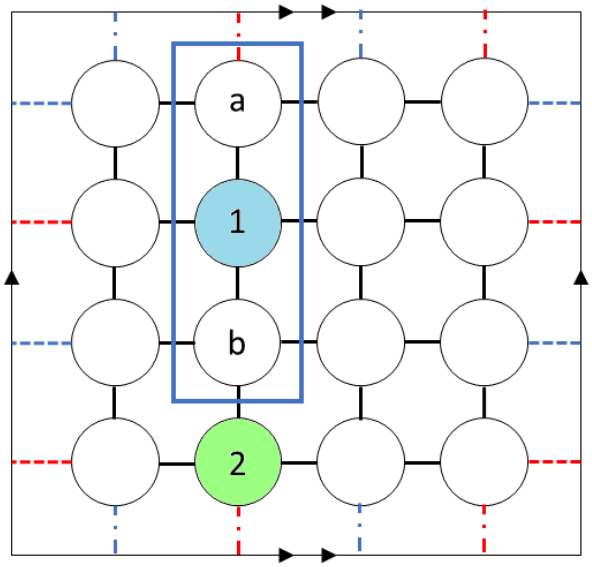

Figure 6: A 3×1 subsystem inside a 4×4 lattice. This subsystem is not convex, while it does represent a rectangle that is typically convex. In this case a and b are connected by two shortest paths with lengths 2. One of these paths does go through the interior of the rectangle, and is denoted by the blue particle 1. Another one passes through green particle 2 at the bottom of the lattice, due to the toroidal topology (22). Thus this shape is not convex, since all shortest paths must strictly contain elements of the subsystem.

one would usually associate with being convex. What happens however when we apply our above-mentioned definition of convex to the toroidal topology? The two particles at the top and bottom are not only at a distance of $N-2$ away from each other, with the path passing through the rectangle, but also a distance of 2, with the path passing through the periodic boundary. This means that for $N \geq 4$ this shape is no longer convex. This isn't exclusive to the rectangle by any means, other classically convex shapes like the square suffer from the same problem.

This somewhat inconvenient property does not necessarily have to be a problem, since it only really occurs for shapes somewhat larger than half the period of the system. Specifically rectangular or square subsystems are not convex if their size in one direction is $L \geq \lceil \frac{N}{2} + 1 \rceil$, where N is the period in that direction and $\lceil \cdot \rceil$ is the ceiling function. The total system size and thus period can be chosen large enough, such that this inequality will not hold. One should however remember that the systems in this paper can not be too large, because even though the operator definition of the Hamiltonian has increased the memory-capacity of the simulation, the computer has still to store the statevector. The required memory for that still increases as $\mathcal{O}(n) = 2^n$ with n the number of particles. In addition there is some other memory limitation concerning the density matrices that is yet to be addressed. The system therefore not be larger than $N \times M = 5 \times 5$.
It is alternatively possible to keep the subsystems-size L small. However, in this case there will not be enough different data-points of subsystems to determine an area-law with reasonable accuracy. As a resolution, in this thesis we will simply stick to shapes that are typically considered to be convex, thus without into taking account the toroidal topology for this. Obviously this will be taken into account when analysing the results.

Now finally, since the original hints of the area-law came from black hole physics, where the boundary is spherical, this paper will firstly focus on the convex shapes that are as spherical as possible. What characterises a sphere is its ratio between the perimeter and the interiors volume, where the boundary-

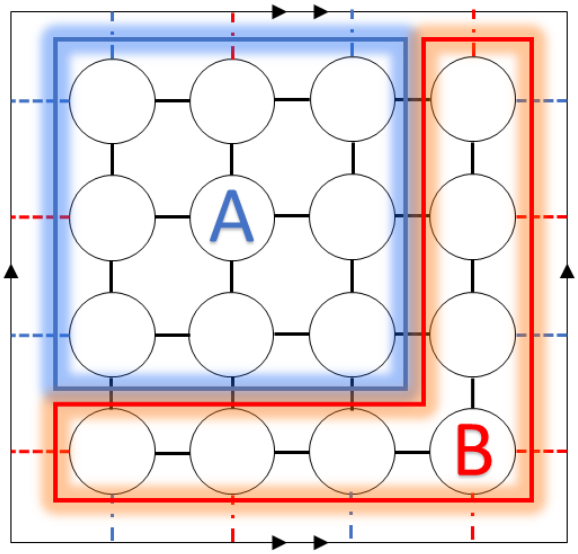

Figure 7: Square subsystem A with sidelength $L = 3$ in a 4×4 lattice. B denotes the complement of A.

area is the smallest possible for a given interior. In our two dimensional discrete situation this means that the shapes must be squares, if we additionally require them to be convex. These shapes will be revered to as the 'roundest' convex shapes, or alternatively just as squares. The boundary-size of these systems $|\partial(A)| = 4L$, where L is the sidelength, and A denotes the subsystem. An example of this can be seen in figure 7 where A has $L = 3$, and B is the complement of A.

The exact algorithm of finding the subsystems is not of real interest[9], but can be found in the code, in Appendix B.

6.2.2 Calculating the Entanglement Entropy of subsystems

Now that the possible subsystems A are determined their entropy needs to be calculated. This is done by applying the equations for the Von Neumann entropy S_N 8 or 9 to the deduced density matrix ρ_A. To make this more precise, let A correspond to the subsystem whose entanglement entropy should be be calculated, and B the complement of A in the total system. Now let $|\psi\rangle \in \mathcal{H}_A \otimes \mathcal{H}_B$ be the groundstate of the Hamiltonian described in (60). Then $\rho_{AB} = |\psi\rangle\langle\psi|$ and $\rho_A = \mathrm{Tr}_B(\rho_{AB})$ and the entanglement entropy of the subsystem A is thus $S_N(A) = \mathrm{Tr}\{\rho_A \ln \rho_A\}$. To perform this calculation the initial total density operator ρ_{AB} needs to be computed in matrix form, which produces the same memory limitations as the Hamiltonian. This is completely unfeasible, even in 'sparse' form as it is not guaranteed that the density operator consists of many zeros. Another method needs to be found, which does not require computing ρ_{AB}.

So it is necessary to calculate the entropy without computing the complete initial density operator ρ_{AB}. It is apparent that this is possible whenever taking a closer look at the actual operations performed. Any pure vector state, thus also the groundstate, can be written as a tensorproduct. So lets write the groundstate as $|\psi\rangle_{AB} = \sum_{i,j} c_{ij} |\chi_i\rangle_A \otimes |\xi_j\rangle_B$, where $|\chi_i\rangle_A \in \mathcal{H}_A$ and $|\xi_j\rangle_B \in \mathcal{H}_B$ denote the i-th and j-th orthonormal basis vectors of Hilbert spaces $\mathcal{H}_A$ and $\mathcal{H}_B$ respectively. The coefficients $c_{ij} \in \mathbb{C}$ depend on $|\psi\rangle_{AB}$, and due to orthonormality of the basis is defined as the inner product $\left(\langle\chi_i|_A \otimes \langle\xi_j|_B\right) |\psi\rangle_{AB}$. It should be noted that our description of $|\psi\rangle_{AB}$ is the most general one in this

[9] It was still very much fun to program, as also this was optimised to be as efficient as possible using different tricks.

Hilbert space, namely as a double sum of orthonormal basis for the separate spaces.
We want to calculate the partial trace over B of the eigenstate $|\psi\rangle\langle\psi|_{AB} = \rho_{AB}$:

$$\begin{aligned}\rho_A &= \mathrm{Tr}_B\, \rho_{AB} \\ &= \mathrm{Tr}_B(|\psi\rangle\langle\psi|_{AB}) \\ &= \mathrm{Tr}_B \left(\sum_{i,j} c_{ij} \, |\chi_i\rangle_A \otimes |\xi_j\rangle_B \sum_{n,m} \bar{c}_{nm} \, \langle\chi_i|_A \, \langle\xi_j|_B \right)\end{aligned} \tag{70}$$

Using the definition of the linear partial trace and subsequently that $|\xi_i\rangle$ forms an orthonormal basis.

$$\begin{aligned}\rho_A &= \sum_{i,j,n,m} c_{ij}\bar{c}_{nm} \, |\chi_i\rangle\langle\chi_n| \, \mathrm{Tr}\{|\xi_j\rangle\langle\xi_m|\} \\ &= \sum_{i,j,n,m} c_{ij}\bar{c}_{nm} \, |\chi_i\rangle\langle\chi_n| \, \delta_{jm} \\ &= \sum_{i,j,n} c_{ij}\bar{c}_{nj} \, |\chi_i\rangle\langle\chi_n|\end{aligned} \tag{71}$$

The evaluation of the trace is thanks to the orthonormality of the basis. It can be seen that the coefficients of the reduced density matrix are just $\sum_j c_{ij} \cdot \bar{c}_{nj}$.
Now if we can determine c_{ij} it is possible to determine the density operator ρ_A by (71). In MATLAB [34] is it is possible to perform the $c_{ij}\bar{c}_{nj} \, |\chi_i\rangle\langle\chi_n|$ operation. This can be found in Appendix C. It is even possible to perform it over all the indices the indices i and n simultaneously. This method of computation requires only storing data as large as the reduced density matrix ρ_A and the original eigenvector. Thus $2^{2dim(A)}$ and $2^{dim(A)+dim(B)}$ complex numbers are required respectively. The problem however is that in some cases $2^{2dim(A)}$ can still be too large to store in memory, especially whenever the number of particles of the subsystem n_A is close to the number in the total system n_{AB}. We can however use the property that $S_N(\rho_A) = S_N(\rho_B)$ by (13), with B being the complement of A in the total system. That way it is possible to only calculate the entanglement entropy of the smaller density matrix without loss of generality, for it is easier to find its eigenvalues. Thus we choose sometimes not to calculate the entropy of the subsystem itself, but rather its complement.

Having calculated the entropy for the different subsystems a method of verifying the area-law (14) has to be constructed. This is done by plotting a first degree polynomial (since the system itself is specially 2 dimensional). This polynomial will pass through the origin, as for the entropy should be zero, if there is no boundary and thus not subsystem. This is not only intuitive, but this entropy should also be equal to the entropy of the total system by the reflexive property (13). Now we know that there are no particles outside the system, by definition, and the groundstate is a pure system. Therefore indeed the total system has zero Von Neumann entropy. The first-degree coefficient will be completely determined by the data-point corresponding to the smallest non-zero boundary. The polynomial will thus not be fitted to the complete data-set. This is because we expect the entropy of the larger subsystems to be disturbed by the periodic boundary of the system (23), leading to non-convex shapes.

6.3 Correlation Length

As mentioned before, due to the periodic boundary conditions, the area-law is more difficult to verify, looking at the entanglement entropy alone. Therefore an additional method to verify the law has been implemented. As mentioned in the theoretical section on entanglement entropy, the area-law is considered to hold true whenever the correlation (16) decays exponentially with length (17).
It is necessary to determine the correlation between all the different points as a function of distance. Let us first look at an example of how to calculate the correlation between some points i and j given

a groundstate $|\psi\rangle$ in practise. In order to use equation (17) some expectation values for the Pauli matrices σ_i^z need to be computed. The convenient thing is that the canonical base-vectors of a the $\frac{1}{2}$-spin statevector $|\psi\rangle$ are exactly the eigenvectors of the σ_i^z operator[10]. The eigenvalues of σ_i^z are namely 1 and -1 for the eigenvectors $|\uparrow\rangle_i = \begin{bmatrix}1\\0\end{bmatrix}$ and $|\downarrow\rangle_i = \begin{bmatrix}0\\1\end{bmatrix}$ respectively. The eigenvalue for $\sigma_i^z\sigma_j^z$ $|\uparrow\uparrow\rangle_{ij}$ and $|\downarrow\downarrow\rangle_{ij}$ is 1 and for $|\uparrow\downarrow\rangle_{ij}$ and $|\uparrow\downarrow\rangle_{ij}$ is -1, all four of which are again basevectors of $|\psi\rangle$. Now using the knowledge on probabilities and considering the expected value is just the sum over all the possible outcomes multiplied by the probabilities, we can easily let MATLAB do these calculations for us.
Furthermore it is necessary to connect these correlations to a distance. Luckily the distance that has already been defined on the lattice, namely the L_1-metric, makes this rather easy for our purposes. It is simply possible to add the horizontal distance d_h to the vertical distance d_v for the particles in consideration. This will produce the total distance $d = d_h + d_v$. One must remember the toroidal topology (22) however. Meaning that, for a lattice that is periodic with period N in the horizontal direction, the horizontal distance between particles with horizontal indices x_i and x_j isn't simply $|x_i - x_j|$ but rather $d_h = \min(|x_i - x_j|, N - |x_i - x_j|)$. The same is obviously true for the vertical case, where the period is denoted by M. Therefore, in order to verify the area-law by relation (17), the initial idea was to fit the correlation was:

$$\left\langle \sigma_i^z ; \sigma_j^z \right\rangle \propto e^{-(\min\{|x_i-x_j|,N-|x_i-x_j|\}+\min\{|y_i-y_j|,M-|y_i-y_j|\})/\xi} \tag{72}$$

The problem with this approach, is that the real meaning of the topology and the periodic boundary condition is overlooked. Namely that some particle at position i in the grid does not only interact with particle j, but also with particle $j + N$ which is identified with j, as well as with $j + 2N$ and so on. Normally this would not be an issue since the limit is taken such that N is large and the interactions would not be significant, but as discussed before this is not the possible memory-wise. To still have a complete analysis of the situation, it is needed to include these periodic interactions as well. It is hypothesised that the expected correlation $\left\langle \sigma_i^z ; \sigma_j^z \right\rangle$ should be proportional to the sum over all these periodic interactions. This notion also makes the use of the $\min\{\cdot\}$ function redundant, somewhat simplifying the equation:

$$\left\langle \sigma_i^z ; \sigma_j^z \right\rangle \propto \sum_{k=-\infty}^{\infty} \sum_{l=-\infty}^{\infty} e^{-(|x_i-(x_j+kN)|+|y_i-(y_j+lM)|)/\xi} \tag{73}$$

This equation can be simplified analytically to remove the double infinite sum[11]. To do so, it is necessary to first choose to which coordinates our x_i and x_j are constrained. Mathematically speaking this means that we are choosing a branch for the x_i and x_j. It will later be apparent why this is important, although it is a technicality that merely the careful reader would have noticed. The branch is chosen such that $0 \leq x_j \leq x_i \leq N - 1$, without loss of generality, and similarly for the vertical coordinates. Now we can start deducing the analytic expression:

[10] Obviously this is no lucky coincidence at all. Most probably σ^z was constructed such that this would be the case
[11] Or as it actually should be referred to: The double doubly infinite series.

$$\begin{aligned}\left\langle \sigma_i^z ; \sigma_j^z \right\rangle &\propto \sum_{k=-\infty}^{\infty} \sum_{l=-\infty}^{\infty} e^{-(|x_i-(x_j+kN)|+|y_i-(y_j+lM)|)/\xi} \\ &= \sum_{k=-\infty}^{\infty} e^{-|x_i-(x_j+kN)|/\xi} \sum_{l=-\infty}^{\infty} e^{-|y_i-(y_j+lM)|/\xi} \\ &= \sum_{k=-\infty}^{\infty} e^{-|x_i-x_j-kN|/\xi} \sum_{l=-\infty}^{\infty} e^{-|y_i-y_j-lM|/\xi}\end{aligned} \tag{74}$$

Since $0 \leq x_i - x_j < N$ and $0 \leq y_i - y_j < M$, we have that $\forall k > 0 \in Z : |x_i - x_j - kN| = -(x_i - x_j - kN)$ and $\forall k \leq 0 \in Z : |x_i - x_j - kN| = x_i - x_j - kN$, with similar equations for y_i. This leads to the following equation:

$$\begin{aligned}\left\langle \sigma_i^z ; \sigma_j^z \right\rangle &\propto \left(\sum_{k=-\infty}^{0} e^{-(x_i-x_j-kN)/\xi} + \sum_{k=1}^{\infty} e^{(x_i-x_j-kN)/\xi} \right) \left(\sum_{l=-\infty}^{0} e^{-(y_i-y_j-lM)/\xi} + \sum_{l=1}^{\infty} e^{(y_i-y_j-lM)/\xi} \right) \\ &= \left(\sum_{k=0}^{\infty} e^{-(x_i-x_j)/\xi} e^{-kN/\xi} + \sum_{k=1}^{\infty} e^{(x_i-x_j)/\xi} e^{-kN/\xi} \right) \\ &\quad \cdot \left(\sum_{l=0}^{\infty} e^{-(y_i-y_j)/\xi} e^{-lM/\xi} + \sum_{l=1}^{\infty} e^{(y_i-y_j)/\xi} e^{-lM/\xi} \right)\end{aligned} \tag{75}$$

Merging the sums for as much components as possible and extracting the common factors:

$$\begin{aligned}\left\langle \sigma_i^z ; \sigma_j^z \right\rangle &\propto \left[e^{-(x_i-x_j)/\xi} + \sum_{k=1}^{\infty} \left(e^{(x_i-x_j)/\xi} + e^{-(x_i-x_j)/\xi} \right) e^{-kN/\xi} \right] \\ &\quad \cdot \left[e^{-(y_i-y_j)/\xi} + \sum_{l=1}^{\infty} \left(e^{(y_i-y_j)/\xi} + e^{-(y_i-y_j)/\xi} \right) e^{-lM/\xi} \right] \\ &= \left[e^{-(x_i-x_j)/\xi} + \sum_{k=1}^{\infty} 2\cosh\left((x_i-x_j)/\xi\right) e^{-kN/\xi} \right] \left[e^{-(y_i-y_j)/\xi} + \sum_{l=1}^{\infty} 2\cosh\left((y_i-y_j)/\xi\right) e^{-lM/\xi} \right]\end{aligned} \tag{76}$$

It is clear from physical considerations that we would wish the correlation length ξ to be positive, since it is to be expected that the correlation drops of with distance. This results in a converging series that the correlation does not blow up[12].
In that case we can evaluate the infinite series, after which we expand the hyperbolic functions, and make single fractions:

$$\begin{aligned}\left\langle \sigma_i^z ; \sigma_j^z \right\rangle &\propto \left[e^{-(x_i-x_j)/\xi} + \frac{2\cosh\left((x_i-x_j)/\xi\right) e^{-N/\xi}}{1-e^{-N/\xi}} \right] \left[e^{-(y_i-y_j)/\xi} + \frac{2\cosh\left((y_i-y_j)/\xi\right) e^{-M/\xi}}{1-e^{-M/\xi}} \right] \\ &\propto \left[\frac{e^{-(x_i-x_j)/\xi} + e^{(x_i-x_j)/\xi} e^{-N/\xi}}{1-e^{-N/\xi}} \right] \left[\frac{e^{-(y_i-y_j)/\xi} + e^{(y_i-y_j)/\xi} e^{-M/\xi}}{1-e^{-M/\xi}} \right]\end{aligned} \tag{77}$$

[12]Which is nice for physical systems What would it mean for the correlation to grow with the distance? I imagine that any particle is maximal entangled with the boundary of a hyperbolic space, cue misplaced Anti-deSitter theories...

Finally, by multiplying both the denominator and numerator of the two fractions by $e^{N/\xi}$ and $e^{M/\xi}$ respectively, we can again simplify into hyperbolic functions:

$$\left\langle \sigma_i^z ; \sigma_j^z \right\rangle \propto \left[\frac{\cosh\left(\frac{2(x_i - x_j) - N}{2\xi}\right)}{\sinh\left(\frac{N}{2\xi}\right)} \right] \left[\frac{\cosh\left(\frac{2(y_i - y_j) - M}{2\xi}\right)}{\sinh\left(\frac{M}{2\xi}\right)} \right] \tag{78}$$

In finding evidence for the area-law, the right-hand side of this equation will be used to fit the correlation function with.
Since this interpretation of the periodic boundary conditions and the hypothesis of the periodic correlation is of our own imagination without being rigorously proven, we should not overfit relation (78). Therefore the fitting function will be have as few free parameters as possible. In order to check the effectiveness of the ansatz however, the periods N and M will be fitted as well even though we know their actual values.
During fitting, the position of the particle i will be taken to be constant, and thus the fit-function of the correlation will be:

$$f(x_j, y_j) = a \left[\frac{\cosh\left(\frac{2(x_i - x_j) - \tilde{N}}{2\xi}\right)}{\sinh\left(\frac{\tilde{N}}{2\xi}\right)} \right] \left[\frac{\cosh\left(\frac{2(y_i - y_j) - \tilde{M}}{2\xi}\right)}{\sinh\left(\frac{\tilde{M}}{2\xi}\right)} \right] \tag{79}$$

Where a, ξ, $\tilde{N}$ and $\tilde{M}$ are fitted to the simulated correlation. For the fit, MATLABs non-robust non-linear least square method will be used with the trust-region method [34]. The code can be found in Appendix D.
Now the reason that we've chosen a branch such that, $0 \leq x_j \leq x_i \leq N - 1$, is that this function is not periodic as the correlation should be. This periodicity was removed when choosing for which k the absolute value $|x_i - x_j|$ would be negative and for which not. To able to do this, some branch has to be chosen.

As a control, the correlation can also be plotted against a periodic reverse polynomial fit. For each of the different first powers of the polynomials, the corresponding equation for the double an infinite sum are given by:

$$\begin{aligned}
\sum_{k=-\infty}^{\infty} \frac{1}{x + Nk} &\rightsquigarrow \frac{\gamma}{\sin(\gamma x)} \\
\sum_{k=-\infty}^{\infty} \frac{1}{(x + Nk)^2} &\to \gamma^2 \csc^2(\gamma x) \\
\sum_{k=-\infty}^{\infty} \frac{1}{(x + Nk)^3} &\to \gamma^3 \cot(\gamma x) \csc^2(\gamma x) \\
\sum_{k=-\infty}^{\infty} \frac{1}{(x + Nk)^4} &\to \frac{\gamma^4}{3} (2 \cot^2(\gamma x) \csc^2(\gamma x) + \csc^4(\gamma x))
\end{aligned} \tag{80}$$

Where $\gamma = \frac{\pi}{N}$ and the first series does not converge on half of its domain, but merely every half period. Different combinations of these periodic functions can be used to fit the eventual simulated correlation functions as a control.

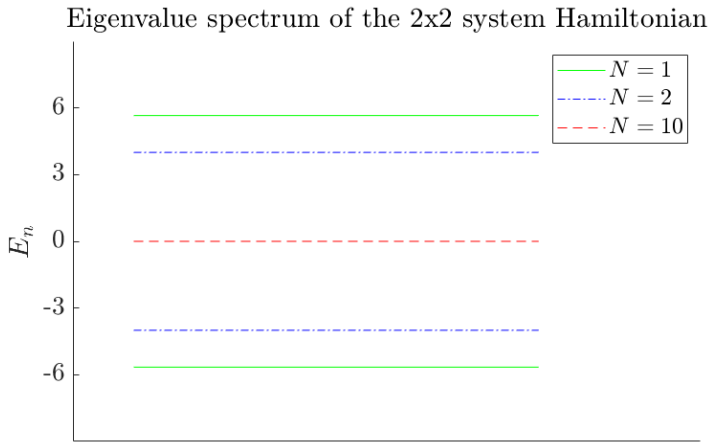

Figure 8: Simple plot of the eigenvalues for the $\hat{H}_{Model}$ Hamiltonian of a 2×2 system. The degeneracies N of the eigenvalues have been denoted by the colour. Eigenvalues $E_n = \pm 5.6568$ are the only non-degenerate eigenvalues. $E_n = \pm 4$ both have degeneracy 2 and $E_n = 0$ has degeneracy 10. In total there are 16 eigenstate.

7 Results of the simulations

In this section the result of the entropy calculations of all the different subsystems, as described in the previous section, are displayed. The section will include the analysis of the eigenvectors of the Hamiltonian, and more specifically of its groundstate and the eigenvalue spectrum. Afterwards the entropy analysis will be made and this will be displayed as a function of the boundary of the subsystem. Finally the correlation function will be analysed and fitted to a periodically extended exponentially decaying function.

7.1 Eigenvectors, groundstate and spectrum

In this subsection, we begin analysing the eigenstates of the system with focus on the groundstate. We do so for constant spin-coupling constants J_{ij} and varying magnetic coupling λ.

7.1.1 Constant Ferromagnetic with no Magnetic Field

Starting of, lets present the results of a system in which the coupling constant is exactly $J_{ij} = 1$ for all i, j. It doesn't matter what the exact factor is, since this factor is independent of the spinsites and is just a scalar factor before the Hamiltonian. This simply corresponds to $\hat{H}_{Model}$ (60), with $\gamma = 0$. This system is to be analysed for multiple square grid-sizes starting with the most simple $N \times N$ system for $N = 2$. This system has dimensionality of $2^4 = 16$, which would make it solvable by hand[13]. This eigenvalue spectrum is visualised in figure 8. Rather than simply including the plot, it might be interesting to see the accuracy of the numerical calculation. For small dimensions like this it is quite possible to do. In table 1 for each computed eigenvalue of a 2×2 system the standard deviation is given. The origin of the standard deviation is due to the power method and is described by the in the previous chapter.
The uncertainty is tiny and is mainly due to numerical precision. No efforts have been taken to make it even smaller, as for further purposes of calculating entropy we are interested in statevectors 'near' the groundstate. It should be noted that the results of the computations are altered depending on the randomness in the statevector with which the power method begins its iterative process.

[13] even though a bit tedious

Table 1: The table for the numerically computer eigenvalues λ of Hamiltonian $\hat{H}_{Model}$ for a 2×2 system. The tiny uncertainty in that computation σ_n is also included. These results are reached after at most $T = 6000$ iterations, or whenever the a uncertainty of $\sigma_n < 10^{-6}$ has been reached. A plot of this spectrum is shown in figure 8

E_n	σ_n
-5.6569	$3 \cdot 10^{-15}$
-4	$7 \cdot 10^{-6}$
-4	$3 \cdot 10^{-6}$
0	$6 \cdot 10^{-6}$
0	$3 \cdot 10^{-5}$
0	$8 \cdot 10^{-6}$
0	$4 \cdot 10^{-6}$
0	$4 \cdot 10^{-6}$
0	$6 \cdot 10^{-4}$
0	$5 \cdot 10^{-6}$
0	$7 \cdot 10^{-6}$
0	$1 \cdot 10^{-5}$
0	$3 \cdot 10^{-6}$
4	$2 \cdot 10^{-6}$
4	$2 \cdot 10^{-6}$
5.6569	$8 \cdot 10^{-10}$

Now that the result for the simple 2×2 case has been shown, we can move on to larger systems. The states are shown in a histogram to give an idea of their Density of States (DoS), displayed in figure 9. The eigenvalues displayed in figure 9(a) are calculated with the power method. These eigenvalue had an uncertainty between $\sigma_1 = 2 \cdot 10^{-14}$ for the lowest eigenvalue and $\sigma_n = 0.6$ for some values. The average uncertainty in the eigenvalues is $\bar{\sigma} = 0.0064$. It has to be noted that the uncertainty of the power method can be made as high as the numerical precision of the computer, although the algorithm will be substantially slower. Due to this uncertainty, the spectrum deviates somewhat from the very precise calculation from MATLAB [34] using the `eig` function, as seen in figure 9(b). The power method produces a good spectral result generally, especially for the lower eigenvalues, and therefore is sufficient for our purposes. Later we will mainly be interested in the groundstate. Looking again at the complete spectrum, one notices the inherit asymmetry, which wasn't present in the 2×2 case. This asymmetry is due to the uneven period of the lattices boundary condition.

For systems from sizes 4×4 it is not possible to compute the complete spectrum using the standard MATLAB algorithms. We will use on these systems and larger. It is therefore of importance to note the uncertainty.

One can see in figure 10 that there is a slight band-structure. The maximum standard deviation of the eigenvalues is $\sigma_{max} = 0.15$ and a mean deviation of $\bar{\sigma} = 0.01$. The bin-width of 0.2 therefore seems to be rather sufficient to capture the spectrum. The lowest eigenvalue at $E_1 = -17.9996$ has standard deviation $3 \cdot 10^{-12}$, which means that the groundstate is more than good enough for our future purpose. Furthermore this groundstate is non-degenerate. In figure 10 merely 237 out of $2^{16} = 65536$ eigenvalues have been portrayed, since the computation is still rather lengthy and computing the entire spectrum of eigenvalues would be not feasible.

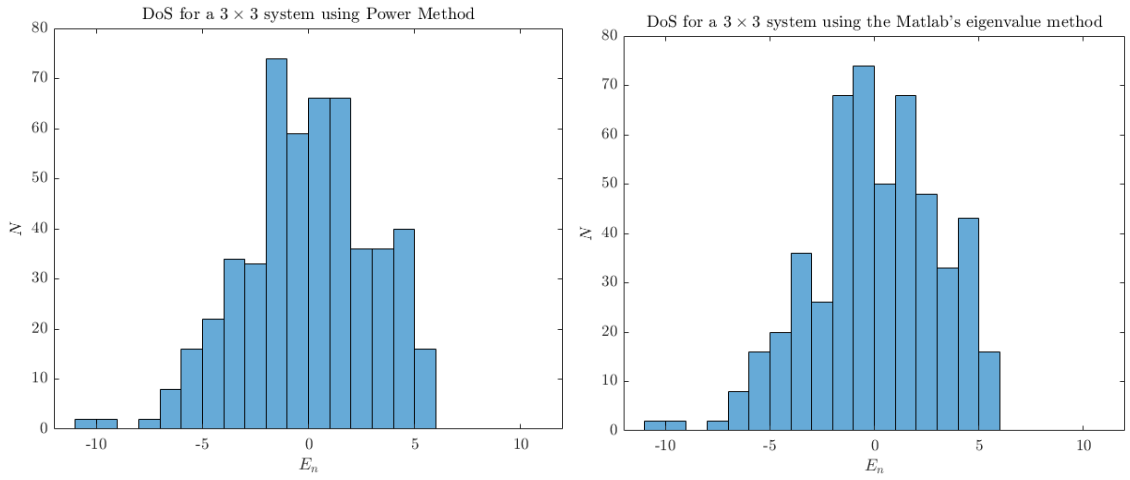

Figure 9: Histogram portraying the degeneracy N for each eigenvalue E_n for the Hamiltonian $\hat{H}_{Model}$ (60) for a 3x3 lattice system. (a) shows these eigenvalues as calculated using the power method and (b) using the `eig` method in MATLAB [34]. The histograms have bins of width 1.

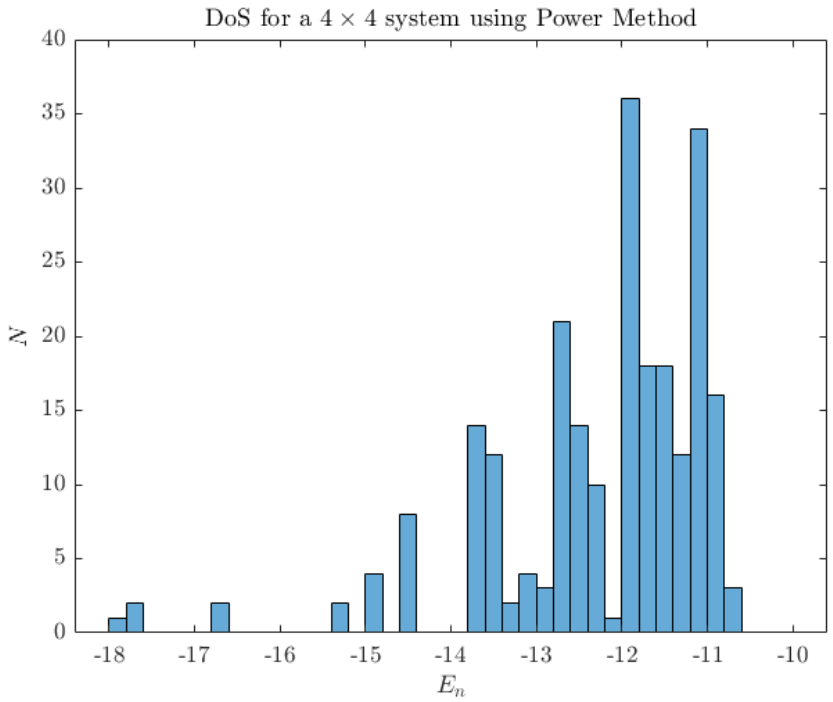

Figure 10: Histogram portraying the degeneracy N and spectrum for each of the lowest 237 out of 2^{16} eigenvalues E_n for the 4x4 lattice system. These eigenvalues are calculated with the power method and have a standard deviation less than $\sigma_{max} = 0.15$. The minimum standard deviation of the eigenvalue is $\sigma_{min} = 10^{-12}$. The average deviation is $\bar{\sigma} = 0.01$. The bins have a width of 0.2.

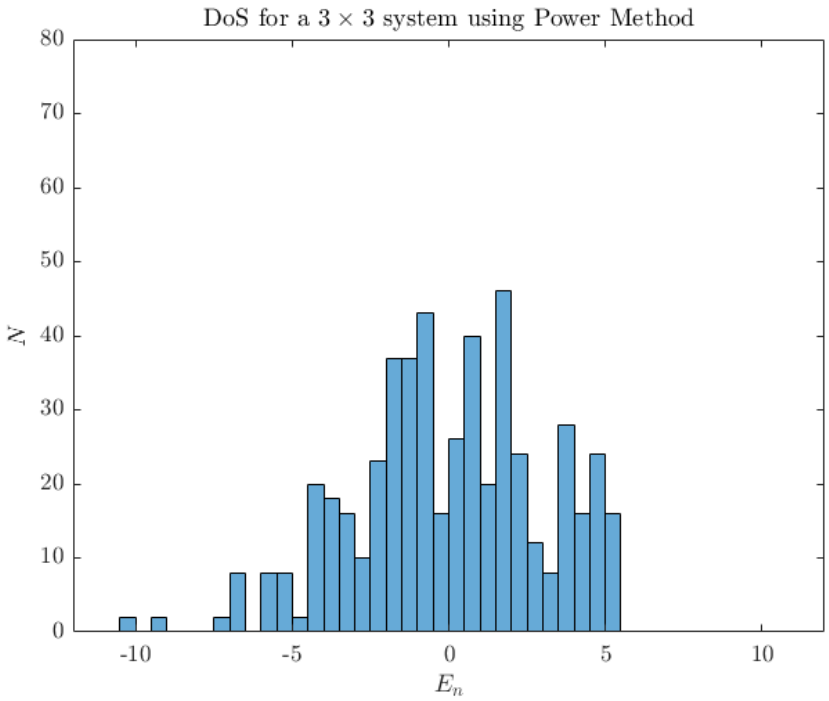

Figure 11: Complete spectrum for magnetic coupling $\lambda = 1$ of a 3×3 lattice. The maximum uncertainty is $\sigma_{max} = 0.2$, smallest uncertainty is below the numerical computer precision and thus to all practical purposes 0. The average uncertainty is $\bar{\sigma} = 0.008$. The binsize is 0.5

7.1.2 Introducing Magnetic Field

Now we share the result after introducing a magnetic field while still keeping the ferromagnetic coupling constant, say $J_{i,j} = 1$. It apart from the sign again does not matter what the exact constant is, since this only adds a scalar factor to the energies and the magnetic interaction. In order to immediately continue with the interesting results we will start with 3×3.

One sees in figure 11 that the spectrum becomes more symmetric as opposed to 9. This trend will continue when increasing the magnetic coupling λ, as one can see in figure 12. One notices that the energy eigenvalues not only spread out more, but the spectrum also becomes more symmetric. As an example the largest eigenvalue is tends closer to the absolute value of the smallest eigenvalue as λ increases.

It takes too long to compute the spectrum for systems of sizes 5×5 and above, for computing a single eigenstate takes about a day on the computer used.

7.2 Entanglement Entropy

Now that one has a good idea of the spectrum computer using the power method and the uncertainty of this computation. We can continue with the groundstate, which is computed to high precision of many negative orders of magnitude, always smaller than 10^{-8}. Therefore we can safely use this eigenvector to compute the entanglement entropy, as this would be sufficiently close to the actual groundstate. The subsystems analysed are generally the round (square), near-convex systems as described in the previous chapter. To remind the reader, the boundary of these sub-systems $|\partial(A)| = 4L$, where L is the side-length of the subsystem, just as one would expect of the squares.

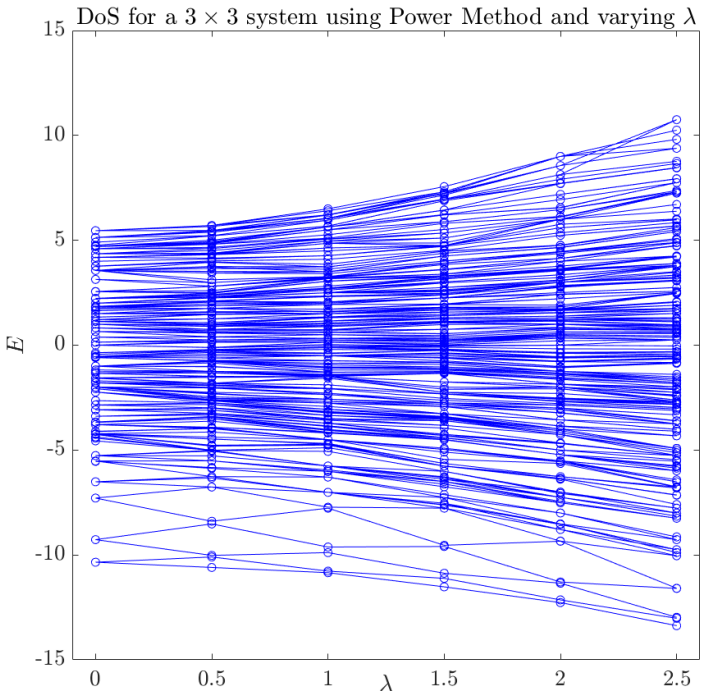

Figure 12: The Density of States (DoS) spectrum for a 3×3 lattice with varying magnetic coupling λ is portrayed. The uncertainty in any eigenvalue is $\sigma_{max} = 0.2$ at most, with the average uncertainty being close $\bar{\sigma} = 0.009$. For each different λ there are 512 different eigenstates.

7.2.1 Constant Coupling

Let us first look at the different subsystems of the systems with total size 4×4 and a constant coupling $J_{ij} = 1$. We will not bother analysing smaller systems, as there are too few square subsystems and therefore too few data-points. For the 4×4 systems there are 3 non-zero data points, making it more reasonable to verify the area-law[14]. For this system we will also change the magnetic coupling, to see its effect. We want to stress that for large subsystems, the subsystem is not strictly convex due to the periodic boundary conditions. For the 4×4 systems, this problem occurs when calculating the entanglement entropy for subsystems with sidelength $L = 3$ and boundary $|\partial(A)| = 12$.

The result for the 4×4 systems can bee seen in figure 13. Here magnetic couplings up to $\lambda = 3$ is taken, since for higher λ the behaviour changes somewhat, as seen in figure 14. Linear fits have been made based on the value of the first non-zero data point. The larger subsystems has not been taken into consideration for this fit, as for those systems the effect of periodicity becomes a significant factor. This is clearly visible in figure 13, where the subsystems corresponding to a boundary area of $|\partial(A)| = 8$ still lie close to the linear fit, but the $|\partial(A)| = 12$ area points lie below it. To quantify this in the case for $\lambda = 0$, the expected entanglement entropy due to the area-law fit $\hat{S}_N$ is displayed against the real entanglement S_N in table 2. This is done for systems of at least $|A| = 8$, as the fit is based on the smaller subsystem. In that table 2, the difference in fitted and actual entanglement $\Delta S_N \equiv \hat{S}_N - S_N$ is plotted. This is as expected, because these subsystems correspond to the subsystems of size $L = 3$, which as discussed before makes them no longer convex due to the boundary conditions. The $|\partial(A)| = 8$, and $L = 2$, data-points however just lie on the edge of being convex. This will be discussed in depth, when analysing the results for the bigger 5×5 system. In figure 2 the entanglement of an excited state $S_{N,\text{excited}}$, and thus not the groundstate, is displayed as well. To be

[14] Although still dubious

Table 2: The calculated groundstate entanglement entropy S_N against the entanglement entropy fitted to the area-law $\hat{S}_N$. This fit is due to the first data-points in figure 13. Finally the entanglement entropy for the 100th out of 65536 excited state $S_{N,\text{excited}}$ is plotted, to show that this excited state does not follow the area-law. The energy of this eigenstate is $E_{100} = -12.1389 \pm 10^{-6}$, in comparison to $E_1 = -17.9996 \pm 4 \cdot^{-12}$. These values are displayed for different boundaries of the subsystems $|\partial(A)|$, all with magntic coupling $\lambda = 0$. The total system size is 4×4.

$\lvert\partial(A)\rvert$	S_N	$\hat{S}_N$	ΔS_N	$S_{N,\text{excited}}$	$S_{N,max}$
8	1.348	1.386	-0.038	2.1408	2.773
12	1.612	2.079	-0.467	3.1373	4.159

more specific, this is the 100th out of 65536 excited state with $E_{100} = -12.1389 \pm 10^{-6}$, in comparison to $E_1 = -17.9996 \pm 4 \cdot 10^{-12}$. It is clearly seen that this state has much higher entanglement entropy than the ground state, showing that it does not follow the area-law, since for $|\partial(A_{\text{excited}})| = 4$ the entanglement entropy is equal for both the groundstate and the excited state, but for higher boundary size, the excited state entropy grows much more rapidly. This shows that the excited state indeed do not follow the area law, as expected. It should be noted that these excited systems also experience a flattening of the entropy whenever the subsystem size approach the total system.
Another interesting note can be made on the ground-state eigenvectors for different magnetic couplings. One notices that although 10 different magnetic couplings λ are plotted, only 8 are portrayed. This is due to the fact that for larger couplings the groundstate eigenvectors tend to overlap. This is already indicative for a transition in the systems behaviour. In this case the $\lambda = 2.25$ and $\lambda = 2.5$ have the same the groundstate eigenvectors, and so have $\lambda = 2.75$ and $\lambda = 3.0$.
One also notices that the entropy is monotonically decreasing up and to $\lambda = 1.5$, slightly rises for $\lambda = 1.75$ and then again drops for $\lambda = 2.0$. This could be attributed to the uncertainty in the eigenvector, as this slightly rises for higher λ. The entropy increase from $\lambda = 2.0$ to $\lambda = 2.25$ seems significant however, and possibly has a relation with the fact that the eigenvectors overlap and some transition is taking place. For $\lambda = 2.75$ and $\lambda = 3.0$ the entropy drops to the lowest point seen so far, and will continue to drop as we will see in later analysis.
Next to that it should be noted, as the magnetic field increases, the area-law seems to hold better, as the fit has a higher R^2 coefficient of determination. This is displayed in table 3. This can be understood as the entanglement entropy converging to a flatter critical state in which the entanglement, as a result of which the fits are artificially better, because the inherit error can not be as large.
Finally, on a general note, it is clear that the entanglement entropy never exceeds the theoretical maximal entanglement entropy of $S_{N,max}(A) = \min\{|A|, |B|\} \log(2)$, where $|A|$ and $|B|$ is the number of the particles in the subsystem and complement respectively. The complement is taken into account due to the reflexive property. However, Whenever $\lambda = 0$ we have for $|A| = 1$ and thus $|\partial(A)| = 4$, that $S_N(A) = |A| \log(2) = \log(2)$, and the particle is maximally entangled. This is true for any state with $\lambda = 0$, as all the interaction in the Hamiltoninian for any particle is due to interactions with other particles, which are not part of that single particle subsystem. For bigger subsystems, this maximal bound is not reached, which is logical due to the area-law 14. The details of this are found in table 2. This bound scales with volume after all $|A| \propto L^d$, which is a higher degree polynomial than the area-law is.

In order to have a better view of the changing qualitative behaviour of the system another plot is made of the 4×4 system with the higher magnetic field strength λ. This plot can be found in figure 14. One sees that from $\lambda = 4.07$ there is zero entanglement entropy, up to computer precision, for any of the subsystems. This will be true for higher λ as well. The pure state is thus product state. It can be understood trivially by noticing that for an enormous magnetic field pointing up, all groundstate the fermion spins want to align with the field. The external magnetic interactions dominate the Hamilto-

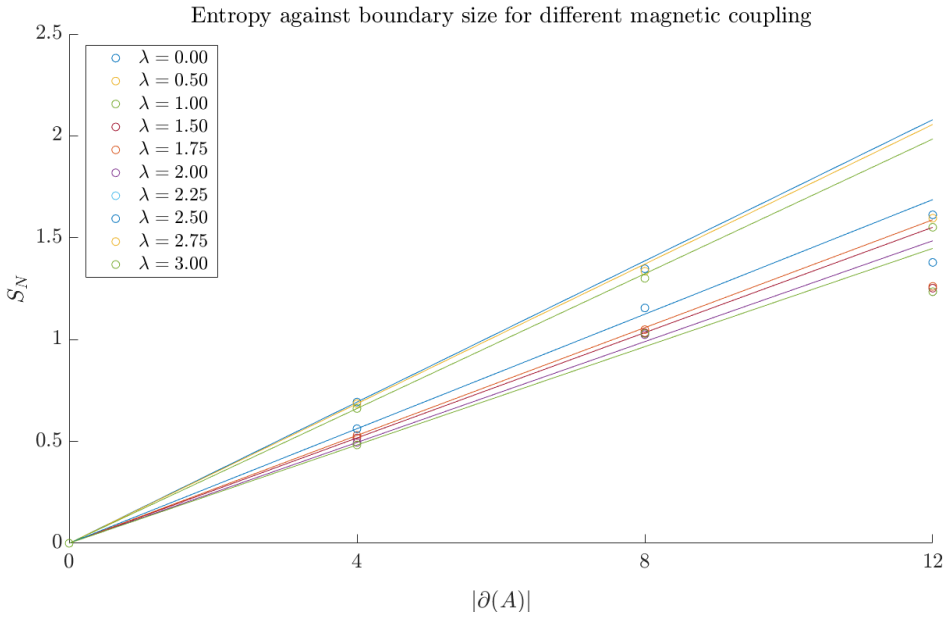

Figure 13: The groundstate entanglement entropy S_N as a function of the boundary of square subsystems $|\partial(A)|$ for different magnetic couplings λ. Linear fits have been made based on the first non-zero area point, $|\partial(A)| = 4$. The lattice size of the total system is 4×4. The straight lines show the area-law based on extrapolating from the first non-zero data point.

Table 3: The R^2 coefficient of determination of the linear fits for the data in figure 13 based on the first data point. It is seen that higher magnetic coupling λ seems to increase the R^2 of the fit.

λ	R^2
0.00	0.8593
0.50	0.8607
1.00	0.8701
1.50	0.9050
1.75	0.8880
2.00	0.9311
2.25	0.9169
2.50	0.9169
2.75	0.9469
3.00	0.9469

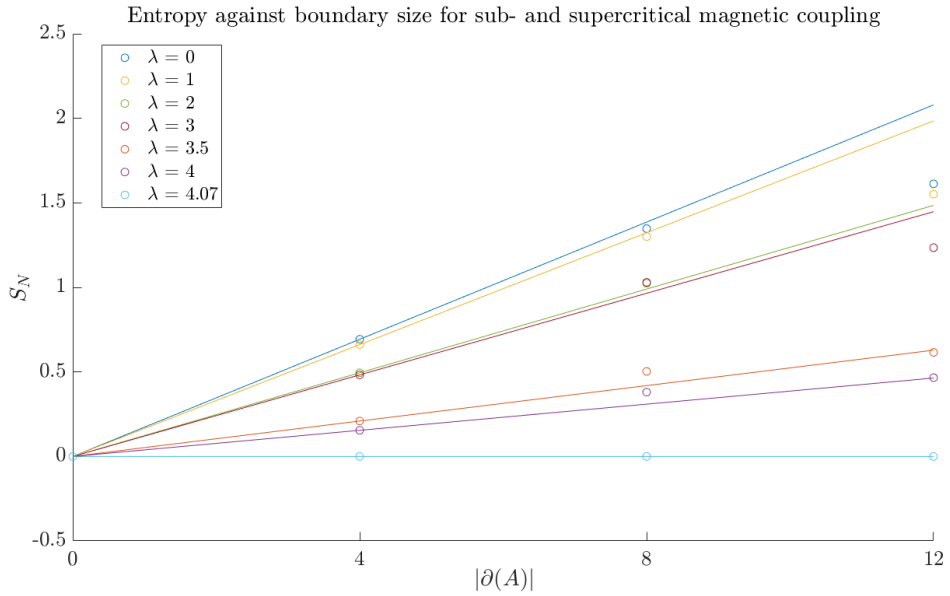

Figure 14: The entropy S_N as a function of the boundary of square subsystems $|\partial(A)|$ at different magnetic fields λ. A area-law fit has been made based on the first non-zero data point. The size of the total system is a 4×4 lattice. For the critical value around $\lambda = 4.07$ the statevector is a product state, with no entanglement entropy for any subsystem.

nian and therefore the state won't be in a superposition. A state which is not in a superposition can not be entangled. Before this critical point however, starting from $\lambda = 3.5$, it can be seen that the area-law fit is not longer an acceptable approximation for the second data point at $|\partial(A)| = 8$, while it seems to come close to the points $|\partial(A)| = 12$. This is somewhat interesting since for $\lambda < 3.5$ the $A = 8$ point was well approximated and the $|\partial(A)| = 12$ has less entropy than the area-law predicts .

7.2.2 5×5 system

For better area-law verification, we want to study the largest possible systems. For one, this gives more data-points to verify the area-law. Perhaps even more useful would be to test the hypothesis that if the system is bigger, the contribution of the correlation resulting from the boundary condition will be smaller. In that case the area-law is expected to hold better for the subsystems of the same size. This is indeed what we have found, as seen in figure 15. The entropy at $|\partial(A)| = 8$ corresponds rather well with the linear fit for the 5×5 systems, as it did for 4×4. One could even argue that the entropy for the 5×5 system fits even better, but this could be due to uncertainty or some other deviation.
What is sure however, is that the entanglement entropy at $|\partial(A)| = 12$ follows the area-law better for 5×5 than for 4×4. This is easily seen as their entropy at $|\partial(A)| = 12$ is equal, but the fit of the 5×5 is closer by. In quantitative terms, when looking at similar data-points, thus up to $|\partial(A)| = 12$, the coefficient of determination R^2 for the 5×5 system is $R^2 = 0.9782$, compared to the $R^2 = 0.8593$ for the 4×4 systems. This gives a strong indication that the deviation from the area-law, which we observe for large subsystems, is due to the system-boundary.

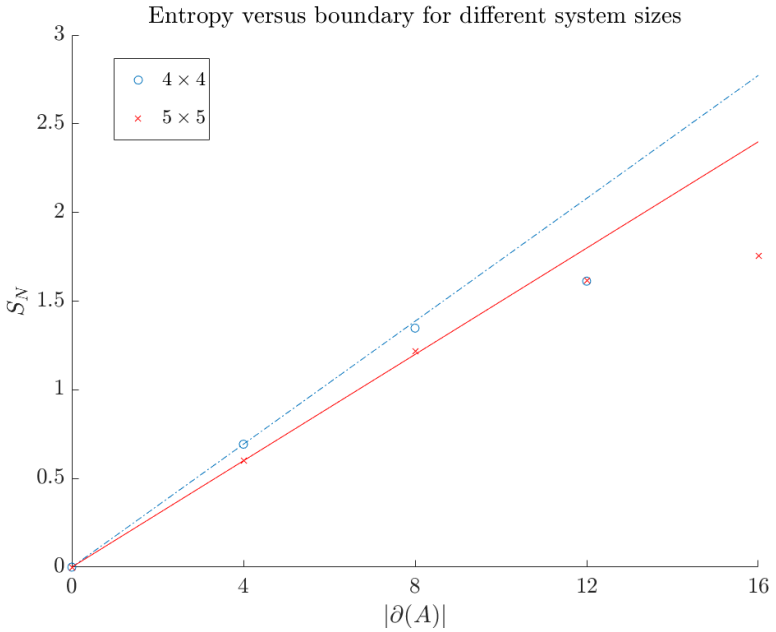

Figure 15: The entropy S_N as a function of the boundary of square $|\partial(A)|$ subsystems at constant magnetic field $\lambda = 0$. The system-size for the round blue data points is 4×4, while it is 5×5 for the red-crossed points. The, respectively blue-dashed and red, lines show the area-law based on the first non-zero data point for boundary $|\partial(A)| = 4$. Their R^2 coefficients of determination are $R^2 = 0.8583$ and $R^2 = 0.9782$ for the 4×4 and 5×5 systems respectively.

7.3 Correlation Length

In this subsection, we will analyse the spin correlation (16) of the different particles in our system. This analysis will be done for the groundstate, as this is where we want to test the area-law. Ultimately we will use equation (79) to fit the correlation. This could also be fitted against the equations in (80), but when one tries to do so with any combination, one quickly finds that this is not a feasible path to follow. For these fits, the uncertainty of any fitparameter is larger that the fitted value of the parameter. Therefore no single fit of this type comes close to the calculated correlation. This indeed can somewhat be expected, as in these situations the correlation tends to infinity at finite values for the distance $|x_i - x_j|$.

Yet when considering the fit of equation (79), the result is striking. Figure 16 displays the correlation for a 5×5 system of particles against plotted the x and y distances between the particles, $|y_i - y_j|$ and $|x_i - x_j|$ respectively. In this distance, the periodic boundary is not taken into account, as this is already represented in the construction of the fit-function. This is fitted using the linear least squares fit. The coefficient of determination for the fit, given by the coefficient of determination, is $R^2 = 0.9846$. The correlation length ξ is given by $\xi = 0.462 \pm 0.001$ and the prefactor $a = -1.49 \pm 0.07$. The periodicity was fitted as $\tilde{M} = 5.00 \pm 0.01$ and $\tilde{N} = 5.00 \pm 0.01$, which in the simulation was exactly $M = N = 5$ and thus in perfect agreement.

In order to give a clearer picture of the correlation, the fit is reduced to a single dimension by taking a single value of $|x_i - x_j|$, for example $|x_i - x_j| = 2$ in figure 17. Any section with 5 data-points would be sufficient however. Obviously, we could also take also pick a value for $|y_i - y_j|$ and keep $|x_i - x_j|$ variable instead. In figure 17 we see clearly that the coefficient of determination for the fit from figure 16 applied to 1 dimension is far from perfect. The $R^2 = -9.4059$ is even negative. However, it is this

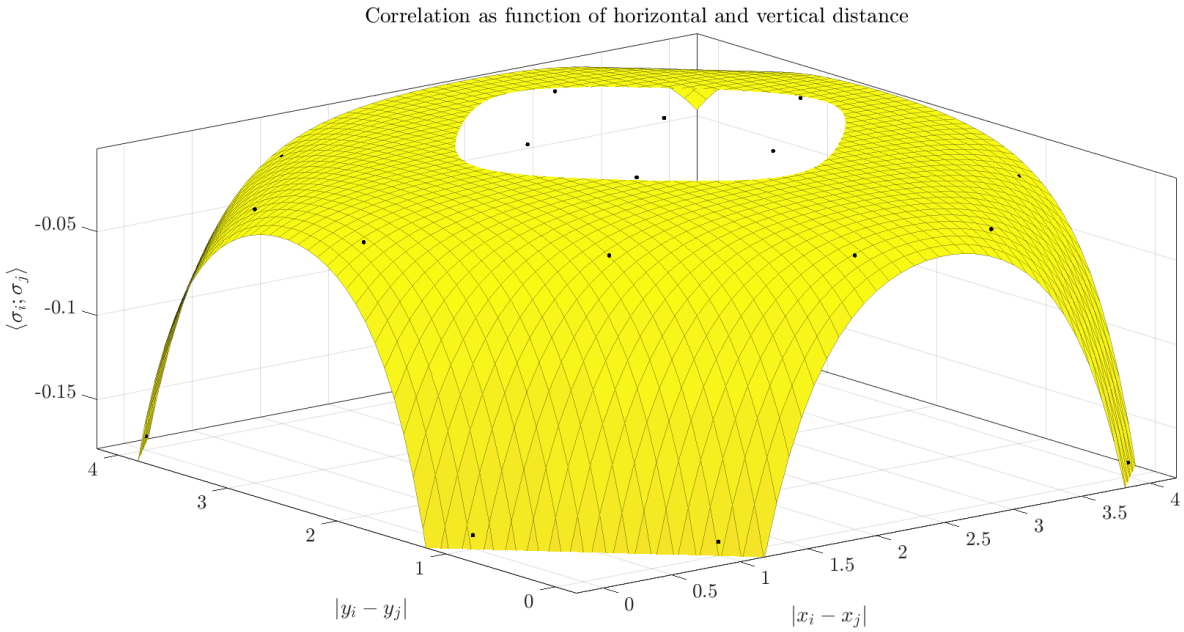

Figure 16: Spin-correlation $\langle \sigma_i; \sigma_j \rangle$ of the groundstate as a function of the horizontal and vertical distances, $|x_i - x_j|$ and $|y_i - y_j|$, between the particles i and j. These are given by the black dots. In yellow, periodically extended function given by equation (79), is fitted. The fit-parameters were $\xi = 0.462 \pm 0.001$, $a = -1.49 \pm 0.07$, $\tilde{M} = 5.00 \pm 0.01$ and $\tilde{N} = 5.00 \pm 0.01$. The resulting R-squared coefficient of determination was $R^2 = 0.9846$. The data-points for the correlation therefore lie beautifully on the fitted surface.

still the same curve that gives the good fit in the whole 2 dimensional space. The effectiveness of this fit-function therefore must be observed in its complete spatial behaviour.

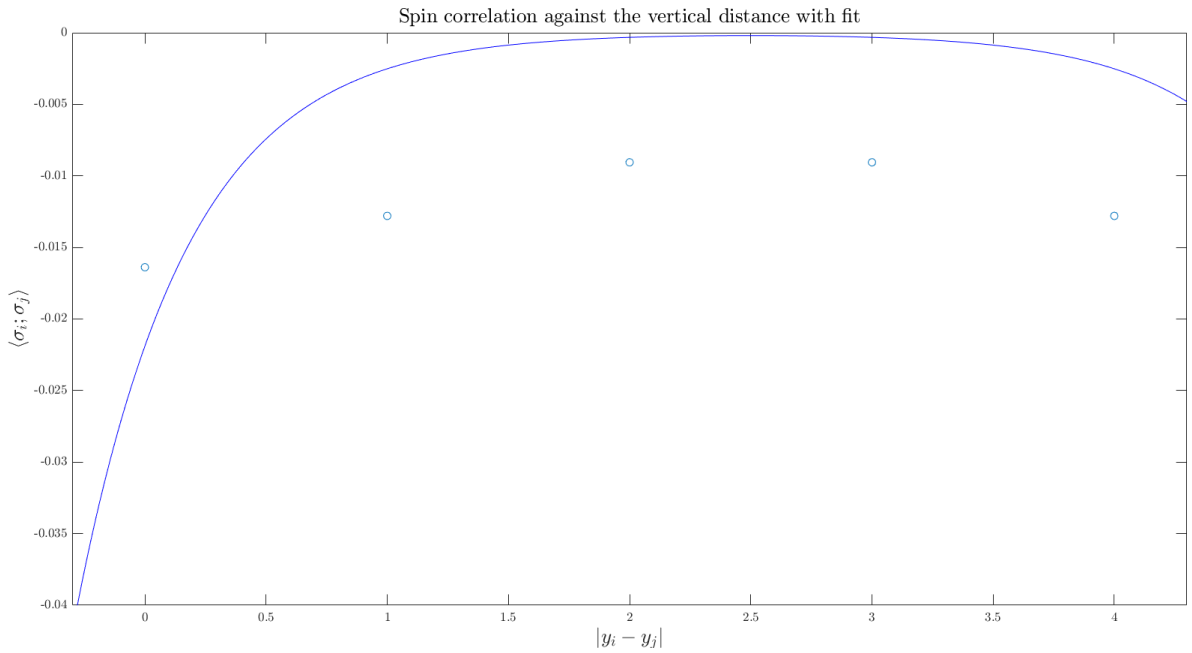

Figure 17: A one dimensional slice through the plot given by figure 16. The slice was taken at $|x_i - x_j| = 2$, as portrayed by the dots. The fit from figure 16 is also displayed by the line. The R^2 coefficient of determination of this fit, applied to the 1 dimensional data-points was negative: $R^2 = -9.4059$. It can be concluded that the fit has no 1D meaning.

8 Discussion and Outlook

8.1 Groundstate and Spectrum

We calculated the, nearest neighbours, XX-model groundstate for the differently sized spin-lattices and different magnetic fields, using the power method. Due to the numerical precision and the dimensionality of our system, the probability of a random vector being orthogonal to the wanted eigenvector is infinitesimal. The power method thus could safely applied. The Hamiltonian used for this can be found in equation (60). It should be noted that in this paper a constant ferromagnetic coupling was analysed.

The power method us allowed to calculate the groundstate for even our largest 5×5 systems of 25 particles, each with 2 complex dimensions. This corresponds to Hamiltonian matrices consisting of $2^{2 \cdot 25} > 10^{15}$ entries. These matrices would take 51GB of RAM to store in the best case, which is more than we have at our disposal. With the power method it even was possible to compute the complete spectrum 3×3 systems and a few hundred eigenstates of 4×4 systems. This however was limited by the computation time, which especially for the systems of 4×4 and larger would not be feasible to compute within a reasonable time. Specifically the 5×5 system, whose dimensionality is thus 2^{25}, it takes a whole day to produce a single eigenvalue on a computing cluster with 16 CPU's, in which a larger cluster could help. The limiting factor for 5×5 is performing the actual Hamiltonian operation. For calculating the spectrum for the 4×4 system, this time complexity is on par with the necessary Gramm-Schmidt orthogonalisation, whose contribution grows enormously whenever the number of eigenvectors computed is large.

It should be noted that when calculating the spectrum, some eigenvectors are rather uncertain. This eigenvector uncertainty based on the standard deviation of some eigenvalues, with the higher being $\sigma_{max} = 0.2$. There does not seem to be a clear prediction which eigenvalues and therefore vectors are uncertain. The uncertainty did not seem to have a clear connection with the degeracy of the state, nor to the eigenvalue it corresponds to. Yet it is not completely random, as choosing different random starting factors results in the similar eigenvectors being uncertain.

8.2 Entanglement Entropy

Addressing the elephant in the room, while it is possible to produce a fit through datapoints to verify the area-law it is still rather sketchy to do so with so few data points. In particular, we've considered 4 unique non-zero square subsystems. The problem is that there is no possibility to look at any larger subsystems, as this would require larger systems, which are not possible to analyse due to computational memory limitations.

We see in figure 15 where entanglement entropy is displayed as a function of the subsystem boundary area $\partial(A)$, it is clear that for the larger subsystems the entropy flattens out. When plotting a line through the entanglement entropy for systems A with sizes the 4×4 and 5×5 , based on the first non-zero datapoint, one sees that this line is still a rather good fit for $|\partial(A)| = 8$, with an error of $|\Delta S_N(A)| = 0.038$. This is a relative error of $|\Delta S_N(A)|/S_N = 2.8\%$. For larger $|\partial(A)|$ the entanglement entropy drops below the area-law predictions, with $|\Delta S_N(A)| = 0.467$ and relative error $|\Delta S_N(A)|/S_N = 29.0\%$. Still, the results are in somewhat good correspondence with the area-law up to $|\partial(A)| = 8$. An alternative to the area-law, perhaps with a logarithmic correction as discussed in the theory or with a volume-law, would produce an even worse fit. For a logarithmic correction or a volume-law, we'd expect entropy values above the area-law. Instead we observe lower values.

In addition a prediction can be made as for the reason why the entanglement entropy flattens out for subsystems is approaching the size of the total system. When this happens, the subsystems are no longer convex, due to the interactions of the subsystem with itself over the periodic boundary. This

has effect on the correlation due to which the entanglement entropy does not necessary correspond to the area-law. It is encouraging that this prediction can be verified to some extent by comparing the results for the systems of sizes 4×4 and 5×5. One sees that subsystems with boundary area $|\partial(A)| = 12$ the entanglement entropy corresponds better to a linear fit for the larger 5×5 system than it does for the smaller 4×4 system. This correspondence is quite significant for the $|\partial(A)| = 12$ systems. For the subsystems of area $|\partial(A)| = 8$ the larger system also seems to produce a better fit, although this is less significant. To be exact, the linear fit for the 5×5 systems had a goodness of $R^2 = 0.9782$, while the 4×4 system fit had a goodness of $R^2 = 0.8593$, when analysing the overlapping data-points. It would be interesting analyse even bigger systems. Yet this does provide a compelling argument in favor of the area-law.

On an interesting note, it is perhaps possible to quantify the entropic relation that one would expect for subsystems whose size approach the total system size. The entropy of a subsystem, is always equal to the entropy of its complement, and for large subsystems could approach the entropy of a 1D subsystem. This is because one could imagine for a large square subsystem that its complement would form a long 1 dimensional row of fermions, and thus have an entanglement entropy given by the relation of such a large row. This is not entirely true, as there still are periodic boundary conditions and there are horizontal and vertical crossing rows. Yet the approximation could work in the limit of a large system. From the results its reasonable to expect the area-law to hold for subsystems up to approximately half the sidelength of the total system, thus as long as they are convex. For larger subsystems it could approach the 1D entropy, although this obviously requires more research.

Finally the entanglement entropy without the external magnetic field, the entanglement entropy S_N never surpassed the maximal possible entanglement entropy $S_{N,max}$. For single particle subsystems it was the case that $S_N = S_{N,max}$ for systems with no magnetic field, and every particle was thus maximally entangled with the rest of the system. This can be expected as in the Hamiltonian every interaction of the single particle is with the rest of the system. When looking at excited states for 4×4 systems, in particular for the 100th out of 65536 excited state for a 4×4 system, we saw that $S_{N,100} \leq S_{N,max}$ with equality for single particle subsystems. For this excited state the entanglement entropy increases substantially quicker than the area-law would predict, which indicates that the area-law is only followed by states sufficiently close to the ground-state. More research is needed to find the exact critical point. It should be noted that whenever the excited subsystems size approached the total system size, their entanglement entropy flattened out a bit as well.

8.3 Changing magnetic field

Now let us discuss the effect of the magnetic field on the entanglement entropy. As one would expect, the groundstate entanglement entropy went down with increasing magnetic field, but not strictly monotonically. For some magnetic field the entanglement entropy was identical, which can be explained by the groundstate not changing with field strength. This is a rather trivial explanation. A more interesting and clear-cut phenomenon however, was that whenever the magnetic coupling was increased from $\lambda/J_{ij} = 2$ to $\lambda/J_{ij} = 2.25$, the entanglement entropy rose significantly. There is possibly some real mechanism making the entanglement entropy not a monotonically decreasing function of the magnetic field. Perhaps it has to do with the change in degeneracy around the states, resulting in more possible states and with it an increase in entropy.

The fact that it is a decreasing function overall still is to be expected, as in the limit that the magnetic coupling is very strong, all the fermionic spins would be aligned with the magnetic field, and there will be no superposition of states. Thus the state can not be entangled and there is no entanglement entropy for any subsystems. The critical point, at which this happens for the 4×4 lattice systems is when the magnetic coupling $\lambda \approx 4.07$, for constant the coupling coefficients is $J_{ij} = 1$.

8.4 Uncertainty in groundstate and entanglement

It is necessary to discuss the link between the uncertainty in the groundstate energy and the uncertainty in the entropy. When the groundstate is computed by the power-method one can test to what extent it really is the groundstate by the spread of the elementwise multiplication-factor after the operation of the Hamiltonian. Ideally this factor should be exactly the eigenvalue. Thus the spread gives a indication of how close the numerically found eigenvalue is close to the real eigenvalue. With this it gives an indication to what extent the found vector is an eigenvector. It however does not necessarily say something qualitatively about the eigenvector uncertainty. To determine the correctness of this eigenvector, it is necessary to have sufficient knowledge of the spectrum, to see what the contribution of the other eigenvectors could be, compared to the own expected eigenvalue. Obviously if there is an eigenvalue very close to the eigenvalue of the groundstate, a vector corresponding to this value could influence the correctness of the computed groundstate-vector.

Still if the correctness of the computed groundstate would be known precisely, it is difficult to verify what this means for the standard deviation of the numerically calculated entanglement entropy. To do this it is necessary to know what the contributions to the entropy of the other eigenvectors that contribute to the groundstate. The uncertainty in the groundstate does therefore not directly translate in the uncertainty of the entropy, and the standard deviation in the expected eigenvalue translates even less.

8.5 Correlation

Let us finally discuss on the analysis of the spin-correlation $\langle \sigma_i; \sigma_j \rangle$. An exponential decay of the spin-correlation indicates the existence of the area law, as can be found in the theory. In order to incorporate the period boudary conditions, this exponential decay is perdiocially extended analytically as seen in equation 78. It is nice to notice that this periodically extension approximates the correlation very well as function of the horizontal and vertical distance of the particles, even when comparing particles close to the boundary. With a coefficient of determination of $R^2 = 0.9846$ and small standard deviation for the fitparameters: the correlation length $\xi = 0.462 \pm 0.001$ and the prefactor $a = -1.49 \pm 0.07$. The periodicity was fitted as $\tilde{M} = 5.00 \pm 0.01$ and $\tilde{N} = 5.00 \pm 0.01$. Thus the conclusion can be drawn that this results are rather significant. The fact that the area-law seems to be validated so clearly here, and not when linearly fitting a function through the entanglement entropy, is because the latter does not take the periodic boundary conditions into account. Therefore in that previous analysis the entanglement entropy is lower than one would expect of the area-law, for subsystems approaching the system size.

It should be noted that the correlation length ξ is rather small, therefore it is conjectured that for larger systems, the entanglement entropy would follow the area-law even if the subsystem would no longer be convex, as long as it is a couple of particles smaller in length than the total system. It seems that 2 particles is sufficient, judging on the analysis of the entanglement entropy for the 4×4 and 5×5 systems, where the S_N for the groundstate followed the area-law very well as long as $L \leq N - 2$, where L is the subsystem size and N the total system size. This can be verified in future research.

8.6 Outlook

It will be to focus on finding critical point for which states the area-law is not longer followed. We know after all that the area-law holds for the groundstate, and doesn't hold for states with a high enough expectation value for the energy, for example excited eigenstates. Perhaps it depends on the contribution of the groundstate to the statevector, based on decomposition. Or maybe merely on the

number of non-groundstate vectors that have some contribution to it. Quite possibly it also depends on which excited state actually contributes, with higher excited states producing violating the area-law more substantially.

It is also paramount to check that the area-law also holds for shapes other than squares. Rectangular shapes should be the primary candidate, as they are convex and it is expected that the area-law holds for them as well. Classically non-convex shapes should be checked as well however. This is bound to give a better understanding of the correlation at the boundary of the subsystems. I expect violation of the area-law for shapes that are non-convex, in which there are some point-pairs whose shortest connecting paths pass strictly outside the shape. Perhaps there can be a area-law like bound, with some correction, depending on how convex the shape exactly is. For shapes whose point-pairs have at least a shortest connecting path passing through the itself, I expect a slight correction to the area-law. This correction could also depend on the convexity.

Another obvious step is to analyse bigger lattice systems by employing more computational memory, which was the limiting factor on size. This will make the periodic boundary less of an issue, and of course the possibility to calculate the entanglement entropy for bigger systems. It should be possible to use non-RAM memory to store the statevectors in chuncks. The biggest problem will be to calculate the reduced density matrix and its eigenvalues, as there is no obvious form to use the power method approach as before. It may be possible to use Schur decomposition.

One could also verify the entanglement entropy for different coupling constants, in particular the anti-ferromagnetic case. The coupling constant can also be varied throughout the lattice, and examined. Also the asymmetric XY-Model can be examined. Both these adaptations should be easily performed within the code in the Appendix, as it requires few changes in the parameters describing the Hamiltoninan operator. The analysis in this paper can subsequently be repeated for those parameters.

Finally it is also interesting to figure out what can be done to decrease the uncertainty in the eigenvalue, when using the power method. One trivial method to increase accuracy is by increasing the computer precision. This obviously increases the necessary storage space. However, we can in any case choose to use the memory more efficiently. Since a good bound to the eigenvalue can be given, it is possible to focus the computational bit-precision on the values where it is needed, instead of their standard full range. That way the accuracy of a float is increased without increasing required storage space. The number of iterations of the power method can also be increased leading to higher precision. Other aspects of the power method could also be tweaked, for example the way that the normalisation is performed could influence the accuracy. Perhaps using the l_∞-norm is not ideal. One could also choose not to normalise every iteration, but every few iterations. This could lead the needed eigenvalues to more quickly explode and being more easily differentiated from the unwanted eigenvalues. A final alteration could be to the cut-off value, at which a number is considered to be zero. This value, which has been introduced order to prevent division by zero-errors or otherwise exploding values due to numerical precision, has been observed to affect the standard deviation of the eigenvalues.

9 Conclusion

In this paper we cautiously conclude for the first time that fermioninic spin-lattices follow the area-law for entanglement entropy in 2 dimensions, with the nearest neighbour, XX-Model Hamiltonian. It is clearly shown that this holds for the groundstate of the system, or at least for states close to it, by comparing this to the behaviour of an highly-excited state. The area-law holds for systems with subcritical magnetic coupling. The conclusion should be taken cautiously however, since it is only checked under certain conditions, namely:

- Constant ferromagnetic coupling $J_{ij} = 1$
- Lattice size up to 5×5
- Square subsystems

Next to these limitations, the periodic boundary of the system made it difficult to test the area-law by looking at the entanglement entropy directly. Subsystems whose size was close to the total lattice size had interaction through the boundary with themselves. This led their entropy to be significantly lower than predicted by the area-law. This became clear when comparing the area-law for similar shapes but varying system sizes. In particular, fitting the area-law for 4×4 lattice systems produced a fit with goodness $R^2 = 0.8593$, while the 5×5 systems produces a fit with a goodness of $R^2 = 0.9782$.
To give an extra indirect validation of the area-law, the spin-correlation was fitting with a periodically extended decaying exponential function in 2 dimensions. This periodic extension was of own design, in order to incorporate the effect of the periodic boundary. The fit was taken over all data-points. This produces a fit goodness of $R^2 = 0.9846$ with a correlation length $\xi = 0.462 \pm 0.001$. From this it can be even more strongly concluded that fermionic systems follow the area-law, and that the earlier deviation from the area-law was indeed due to the system boundary.
While this area-law validation is given only for square systems and ferromagnetic coupling, it is expected to hold for rectangular systems and anti-ferromagnetic coupling as well.

References

[1] Max Planck. On the theory of the energy distribution law of the normal spectrum. *Verhandlungen der Deutschen Physikalischen Gesellschaft*, 273, 1900.

[2] A. Einstein. Über einen die Erzeugung und Verwandlung des Lichtes betreffenden heuristischen Gesichtspunkt. *Annalen der Physik*, 322:132–148, 1905.

[3] N. Bohr. I. on the constitution of atoms and molecules. *The London, Edinburgh, and Dublin Philosophical Magazine and Journal of Science*, 26(151):1–25, 1913.

[4] Léon van Hove. Von Neumann's contributions to quantum theory. *Bulletin of the American Mathematical Society*, 64:95–99, 1958.

[5] E. Schrödinger. *Collected Papers on Wave Mechanics*. AMS Chelsea Publishing Series. AMS Chelsea Pub., 2003.

[6] H. Wimmel. *Quantum physics and observed reality: A critical interpretation of quantum mechanics*. 1992.

[7] Brian C. Hall. *Quantum Theory for Mathematicians*. Springer-Verlag, 1 edition, 2013.

[8] E. Noether. Invariante variationsprobleme. *Nachrichten von der Gesellschaft der Wissenschaften zu Göttingen, Mathematisch-Physikalische Klasse*, 1918:235–257, 1918.

[9] D.J. Griffiths. *Introduction to Quantum Mechanics*. Pearson international edition. Pearson Prentice Hall, 2005.

[10] G.J. Murphy. *C*-Algebras and Operator Theory*. Elsevier Science, 1990.

[11] David Bohm. A suggested interpretation of the quantum theory in terms of "hidden" variables. *Phys. Rev.*, 85:166–193, Jan 1952.

[12] Michael A. Nielsen and Isaac L. Chuang. *Quantum Computation and Quantum Information: 10th Anniversary Edition*. Cambridge University Press, New York, NY, USA, 10th edition, 2011.

[13] R. Clausius. Ueber die bewegende kraft der wärme und die gesetze, welche sich daraus für die wärmelehre selbst ableiten lassen. *Annalen der Physik*, 155(3):368–397, 1850.

[14] W. Pauli and C.P. Enz. *Statistical Mechanics*. Dover Books on Physics Series. Dover Publications, 2000.

[15] C. E. Shannon. A mathematical theory of communication. *The Bell System Technical Journal*, 27(3):379–423, July 1948.

[16] Alfréd Rényi. On measures of information and entropy. *Proceedings of the fourth Berkeley Symposium on Mathematics, Statistics and Probability*, page 547–561, 1961.

[17] Erik Verlinde. On the origin of gravity and the laws of newton. *Journal of High Energy Physics*, 2011, 01 2010.

[18] Mark Srednicki. Entropy and area. *Phys. Rev. Lett.*, 71:666–669, Aug 1993.

[19] S. W. Hawking. Particle creation by black holes. *Comm. Math. Phys.*, 43(3):199–220, 1975.

[20] J. Eisert, M. Cramer, and M. B. Plenio. Colloquium: Area laws for the entanglement entropy. *Rev. Mod. Phys.*, 82:277–306, Feb 2010.

[21] G. Vidal, J. I. Latorre, E. Rico, and A. Kitaev. Entanglement in quantum critical phenomena. *Phys. Rev. Lett.*, 90:227902, Jun 2003.

[22] José Ignacio Latorre, E. Rico, and G. Vidal. Ground state entanglement in quantum spin chains. *Quantum Information & Computation*, 4(1):48–92, 2004.

[23] M. B. Plenio, J. Eisert, J. Dreißig, and M. Cramer. Entropy, entanglement, and area: Analytical results for harmonic lattice systems. *Phys. Rev. Lett.*, 94:060503, Feb 2005.

[24] Michael M. Wolf. Violation of the entropic area law for fermions. *Phys. Rev. Lett.*, 96:010404, Jan 2006.

[25] J. P. Keating and F. Mezzadri. Entanglement in quantum spin chains, symmetry classes of random matrices, and conformal field theory. *Phys. Rev. Lett.*, 94:050501, Feb 2005.

[26] J. I. Latorre and A. Riera. A short review on entanglement in quantum spin systems. *Journal of Physics A: Mathematical and Theoretical*, 42(50):504002, dec 2009.

[27] Fernando G. S. L. Brandão and Michal Horodecki. An area law for entanglement from exponential decay of correlations. *Nature Physics*, 9:721 EP –, Sep 2013. Article.

[28] S. Sachdev. *Quantum Phase Transitions*. Cambridge Univ. Press, 1999.

[29] P. Christe and M. Henkel. *Introduction to conformal invariance and its applications to critical phenomena*. Springer-Verlag, 1 edition, 1999.

[30] A. Dutta B. K. Chakrabarti and P. Sen. *Quantum Ising phases and Transitions in Transverse Ising Models*. Springer-Verlag, 1 edition, 1996.

[31] G. C. Wick. The evaluation of the collision matrix. *Phys. Rev.*, 80:268–272, Oct 1950.

[32] U. Fano. Description of states in quantum mechanics by density matrix and operator techniques. *Rev. Mod. Phys.*, 29:74–93, Jan 1957.

[33] B.-Q. Jin and V. E. Korepin. Quantum spin chain, toeplitz determinants and the fisher—hartwig conjecture. *Journal of Statistical Physics*, 116(1):79–95, Aug 2004.

[34] The MathWorks Inc. Matlab and statistics toolbox. 2018b.

[35] Alioscia Hamma, Radu Ionicioiu, and Paolo Zanardi. Bipartite entanglement and entropic boundary law in lattice spin systems. *Phys. Rev. A*, 71:022315, Feb 2005.

Appendices

A MATLAB: Finding the spectrum and groundstate

In this Appendix the code to compute the spectrum, and with it the groundstate, is displayed. The code, which is written in MATLAB [34], consists of several parts. The main part is used to run the power method, to find as much eigenvectors as desired. This main part calls on multiple functions. Some as simple as calculating the norm, but also functions defining the lattice topology and the Hamiltonian operator.

Lets first display the main part:

```
%% Finding the Spectrum of Eigenvectors

clear;
close all;

corr_rng = 130;
rng(corr_rng)

M=4;
N=4;
%MxN Matrix
Nqubits= N*M;

%Define the neighbours (topology)
neighbourM = neighbourMatrix(M,N); %M x N x (2*N*M) Matrix with in
    each layer to pairs of neighbours, periodically as well
checkT = neighbourM;
checkT = reshape(checkT,[N*M,size(checkT,3)]);  %N*M x 2*N*M Matrix,
    with in each column the pairs

%Initialising some variables used later
N_stdLoop = 1;
N_EigV = 4;
E_nAll = zeros(N_EigV,N_stdLoop);
Sig_nAll = zeros(N_EigV,N_stdLoop);
stdList = 0.1*((1:N_stdLoop)-1);
projectionM = sparse(2^Nqubits,2^Nqubits);


%Define Coupling Coefficients
mu = 1;
std = 0;
Corr = mu+std*randn(2*M*N,1);%ones(2*M*N,1); %Normally distributed
    coupling coefficients


%Define Hamiltonian interactions
yInteract = true;
gamma = 0;
magneticInteract = true;
```

```
lambda = 0;
const = 10; %Basic energy subtracting from Hamiltonian to get the most
    negative Eigenvalue as the largest absolute one
T = 6000; %Number of times that the Powermethod is repeated at

%Initialising some variables used later
completePsi = [];
E_n = zeros(N_EigV,T);
E_nFin = zeros(N_EigV,1);
Sig_n = zeros(N_EigV,T);
Sig_nFin = zeros(N_EigV,1);
maxabsDiff = zeros(N_EigV,T);
maxAcc = zeros(N_EigV,T-1);

for l = 1:N_EigV %Spectrum Loop

    Psi0 = rand(2*ones(1,N*M),'double');%+single(1i)*rand(2*ones(1,N*M
       ),'single'); %Although we expect real eigenvector, a complex
       linear combination of them is possible
    Psi0 = 2*Psi0-1;
    Psi0 = Psi0/mean(abs(Psi0(:))); %M*N dimensional normalized vector
    PsiNew = Psi0;

    stopping = 0;
    n = 1;

    while not(stopping) %Powermethod Loop per eigenvector
        %{
            if l > 1
                PsiNew = PsiNew-reshape(projectionM*straightenedPsi,
                   size(PsiNew));
            end
        %}

        %Perform Gramm-Schmidt
        if(mod(n,1)==0)
            for prevEigVCount = 1:l-1
                prevEigV_straight = completePsi(:,prevEigVCount);
                component = prevEigV_straight'*reshape(PsiNew,size(
                   prevEigV_straight));
                prevEigV = reshape(prevEigV_straight,size(PsiNew));
                PsiNew = PsiNew-component*prevEigV;
            end
        end
        PsiOld = PsiNew;

        %Perform Hamiltonian
        PsiNew = Hamiltonian(PsiOld,checkT,Corr,const,yInteract,gamma,
           magneticInteract,lambda); %Acting on PsiOld with
           Hamiltonian defined by Correlation factor, and whether y-
           interactions are taken into accoutn

```

```
82          %Post-conditioning for each iteration:
83          %Normalising, cutting off small numbers, check stopping-
                conditions
84          if  mod(n,1) == 0
85              nonZeroAfterHam = PsiNew.*(abs(PsiNew)>10^-6);
86              temp = PsiOld.*(abs(PsiOld)>10^-4); %The higher the cutoff
                    , the better the result oftentimes for some reason
87              EigSpread_n = nonZeroAfterHam.*temp./(temp.^2);
88              EigE_n = real(EigSpread_n); %Taking the real values,
                    because they must be real
89              E_n(l,n) = nanmean(EigE_n(:))+const;
90              Sig_n(l,n) = nanstd(EigE_n(:));
91
92              absDiff = abs(PsiNew-E_n(l,n)*PsiOld);
93              maxabsDiff(l,n)=max(absDiff(:));
94
95              if n>1
96                  maxAcc(l,n-1)=(maxabsDiff(l,n)-maxabsDiff(l,n-1));
97                  if ((maxabsDiff(l,n)-maxabsDiff(l,n-1))== 0) %Stop if
                        no progress
98                      disp('No progress')
99                      stopping =1;
100                 end
101
102                 if Sig_n(l,n-1)<10^-5 %Stop if good eigenvalue
103                     disp('Good Enough')
104                     stopping=1;
105                 end
106
107                 PsiNew = PsiNew/max(abs(PsiNew(:))); %Normalising in
                        each step
108             end
109             if n==T
110                 stopping =1;
111             end
112         end
113
114         difference = abs(PsiOld-PsiNew); %Recheck progress
115         stopping = stopping||not(logical(sum(difference>10^(-9),'all')
                ))||(n>T);
116
117         if  mod(n,250) == 0
118             fprintf("This is the %dth iteration of the %dth
                    eigenvector for the %dth standard deviation\n",n,l,
                    stdLoop)
119             stopping = not(logical(sum(difference>10^(-9),'all')))+(n>
                    T);
120         end
121         n = n+1;
122     end
123     normPsi=dNorm(PsiNew);
124     PsiNew = PsiNew/normPsi; %Normalizing
```

```
125
126     % Randomize:
127     straightenedPsi = reshape(PsiNew,[numel(PsiNew),1]);
128     straightenedPsi = straightenedPsi.*(abs(straightenedPsi)>10^-16);
129     completePsi =[completePsi,straightenedPsi];
130     E_nFin(l,1) = E_n(l,n-1);
131     Sig_nFin(l,1) = Sig_n(l,n-1);
132     %projectionM = projectionM+straightenedPsi*straightenedPsi';
133 end
134
135 E_nAll(:,stdLoop) = E_nFin(:,1); %Display expected eigenvalue progress
136 Sig_nAll(:,stdLoop) = Sig_nFin(:,1); %Display deviation eigenvalue
       progress
137
138 %Save useful values
139 c = clock;
140 savename = strcat('BEPRunSpectrum','_h',mat2str(c(4)),'_m',mat2str(c
       (5)),'_s',mat2str(c(6)),'.mat');
141 save(savename,'corr_rng','gamma','mu','stdList','E_n','E_nAll','
       Sig_nAll','M','N','completePsi','lambda','gamma');
```

Now it is needed to display the functions called by the main part. These will be, in order, the function for the l_2 vectornorm, the functions determining the topology and the function executing the Hamiltonian operation.

```
1 function norm = dNorm(psi)
2 %%% Calculating the standard l2 vector-norm
3
4 psi = reshape(psi,[numel(psi),1]);
5 norm = sqrt(psi'*psi);
6 end
```

```
1  %% Lattice Topology
2
3  function neighbourM = neighbourMatrix(M,N)
4  %%% Define full topology
5
6  neighbourM = zeros(M,N,2*N*M);
7
8  checkMN = sideNeighbourhood(M,N);
9  checkNM = sideNeighbourhood(N,M);
10 checkNM = permute(checkNM,[2,1,3]);
11 if ~isequal(checkMN,checkNM) %In case M or N are 1 and we'd expect to
       have self-interaction, but due to the definition, we get side-
       iteraction. It's ok to delete one, since the self-interaction would
        just result in an identity Hamiltonian in that direction.
12     neighbourM(:,:,1:N*M) = checkMN;
13     neighbourM(:,:,N*M+1:end) = checkNM;
14 else
15     neighbourM = checkMN;
16 end
17
```

```
18
19  end
20  function sideNeighboursM = sideNeighbourhood(M,N)
21  %%% Define topology in one direction
22
23  sideNeighboursM = zeros(M,N,N*M);
24  sideNeighboursM(1:2) = [1;1]; %Set two neighbours. Does NOT work if M
        is 1!!
25  for i = 2:M
26      sideNeighboursM(:,:,i) = circshift(sideNeighboursM(:,:,i-1),1,1);
            %Create all the combinations in the First Column
27  end
28  for i = 1:N-1
29      sideNeighboursM(:,:,i*M+1:(i+1)*M) = circshift(sideNeighboursM
            (:,:,1:M),i,2); %Shift the first column to the right
30  end
31  end
```

```
1   function HPsi = Hamiltonian(Psi,checkT,Corr,const,yInteract,gamma,
        magneticInteract,lambda)
2   %%% Executing the Hamiltonian operation
3
4   HPsi = zeros(size(Psi)); %Will be the vector after applying the
        Hamiltonian
5   numDim = numel(size(Psi));
6
7   %Define interaction between two neighbours with factors
8   face2D = (ones([1,1,2*ones(1,numDim-2)]));
9   if yInteract
10      scalingFactorProto = [gamma*face2D 1*face2D;1*face2D gamma*face2D
            ];
11  else
12      scalingFactorProto = [face2D face2D;face2D face2D];
13  end
14
15  %Define external magnetic interaction
16  face1D = ones([1,2*ones(1,numDim-1)]);
17  if magneticInteract
18      magneticScaling = [face1D; -face1D];
19  end
20
21  %Perform all neighbours interaction
22  zerosTemplate = zeros(1,numDim);
23  for i =1:size(checkT,2)
24      %Define which two neighbours are interacting
25      connected = find(checkT(:,i));
26      backPermute = zerosTemplate;
27      backPermute(connected(1)) =1;
28      backPermute(connected(2)) =2;
29      backPermute(backPermute==0)=3:numDim;
30
31      %Make sure the interaction is performed on those neighbours
```

```
32      scalingFactorApplied = permute(scalingFactorProto,backPermute);
33
34      %Perform that interaction by scaling and flipping the spins
35      HPsi = HPsi - Corr(i)*flip(flip(Psi,connected(1)),connected(2)).*
            scalingFactorApplied;
36  end
37
38  %Performing all external magnetic interactions
39  for i = 1:numDim
40      backPermute = zerosTemplate;
41      backPermute(i) = 1;
42      backPermute(backPermute==0) = 2:numDim;
43      HPsi = HPsi + 0.5*lambda*Psi.*permute(magneticScaling,backPermute)
            ;
44  end
45
46  %Subtract constant energy in order to get the lowest eigenvalue
47  HPsi = (HPsi-const*Psi);
48  end
```

B MATLAB: Determining the subsystems

Having found the groundstate, it is not yet possible to compute the entanglement entropy. First it is necessary to find the (square) subsystems whose entropy will be calculated. In this Appendix, the code responsible for that algorithm will be outlined. The specific code is used for total systemsize of 5×5, but can easily be transformed into other systemsizes. In addition, not just square subsystems can be found, but any subsystems that have an optimal boundary to interior ratio for their interior-size. The code will also use the topology functions described in Appendix A. Not only the subsystems are found, but also their complement.

```
clear; close all;
M=5;
N=5;
%MxN Matrix

neighbourM = neighbourMatrix(M,N); %M x N x (2*N*M) Matrix with in each layer to pairs of neighbours, periodically as well
checkT = neighbourM;
checkT = reshape(checkT,[N*M,size(checkT,3)]);

%For 5x5 Handwritten optimal A
vToAOptimal = [4 0 0 8 0 0 0 0 12 0 0 0 0 0 0 16 0 0 0 0 0 0 0 0 0];
NPerm = M*N*(min(M,N)-1); %Total different permutations, not counting the 0
allPerm = zeros(NPerm,M,N);
V = zeros(1,NPerm);
A = zeros(1,NPerm);

for i = 1:min(N,M)-1
    for j = 1:N*M
        Bx = (N-mod(-((N-mod(-j,N))+[0:i-1]),N)); %Make the displacement in the x-direction
        By = N*mod(floor((j-1)/N)+[0:i-1],N); %Make y-displacement (starting with 0 on top row)
        B = By'+Bx; %Combine the displacements to get all the different possibilities, as one would want
        B = reshape(B,[numel(B),1]);

        choosing = zeros(1,N*M);
        choosing(B) = 1;

        allPerm(N*M*(i-1)+j,:)=choosing; %Assign these choices to the big table
        V(N*M*(i-1)+j)=numel(B); %Calculate Volume
        choosingBitMap = repmat(choosing',[1,size(checkT,2)]); %repeat the choosing, in order to compare with all the different neighbour combination
        overlap = choosingBitMap.*checkT; %See which ones overlap
        inward = sum((sum(overlap,1)==2)); %Check which ones has to overlapping bits -> those are neighbours
        A(N*M*(i-1)+j)=4*numel(B)-2*inward; %Calculate area
    end
```

```
end
allGood = [allPerm;~allPerm]; %Since in this case everything is
   programmed and all are good.
allGood = reshape(allGood,[size(allGood,1),N*M]);
VGood = [V,N*M-V];
AGood = [A,A];

biggestV = N*M; %Biggest volume discussed
setList = cell(2,biggestV); %Make list for each volume

for i = 1:biggestV

    perms_perV = VGood==i; %Logical with only the entries
       corresponding to the right volume
    idxV = find(perms_perV); %And their indices
    numPerms = numel(idxV); %And their total number
    ListForV = cell(2,numPerms); %Making a cell-array for those
       permutations for each specific volume
    for j = 1:numPerms
        ListForV{1,j} = allGood(idxV(j),:); %Include the choosing
        ListForV{2,j} = AGood(idxV(j)); %Area
    end
    setList{1,i} = ListForV; %Assign the permutation list per volume
       in the complete list
    setList{2,i} = i; %Assign the permutation list per volume in the
       complete list
end

save('round_5x5','setList'); %Save the complete list
```

C MATLAB: Calculating the entanglement entropy

Now that the subsystems and groundstate is calculated, the entanglement entropy of each subsystem can be calculated. This is done in a main programm, which loads this precalculated groundstate and subsystems. It performs the calls the function that performs the partial trace over each of the subsystems or its complement.

The main part of the code is:

```
load('eigenvector_5x5_4000N')
load('round_4x4.mat')
rng('shuffle')

S = complex([]);
V = [];
A = [];

%Defining the cut-off, from which sizes the complement will be
    calculated
%instead of the system itself:
safetyFactor = int64(floor(N*M/2));

for i = 1:size(setList,2) %Loop through all the subsystem sizes
    %i
    ListForV = setList{1,i};
    for j = 1:size(ListForV,2) %Loop through the subsystems with that
        size

        choosing = ListForV{1,j}; %What indices are the subsystems
        allPart = 1:N*M;
        B = allPart(logical(choosing)); %What qubits do these
            correspond to
        if N*M-i<=safetyFactor %Calculate only if the system is
            suitable size
            densityA = partialTraceB(PsiEigV_hil,N*M,B); %Compute
                partial Trace
            eigD = eig(densityA); %Compute eigenvalues of reduced
                density matrix
            eigD = eigD(abs(eigD)>10^(-8));
            V = [V,i];
            A = [A,ListForV{2,j}];
            S=[S -sum(eigD.*log(eigD))]; %Compute the entropy
        end
    end
end
S = S(V~=0);
A = A(V~=0);
V = V(V~=0);

c = clock;
if saving
    savename = strcat('Entropy_Volume','_h',mat2str(c(4)),'_m',mat2str
```

```
        (c(5)),'_s',mat2str(int8(c(6))),'.mat');
    save(savename,'S','V','A','M','N','corr_rng','lambda','gamma','
        Corr');
end
```

The function describing the partial trace calculations is given by:

```
function densityMatrix = partialTraceB(psi,totDim,tracingDim)
%%% Partial Trace computation

%Noting dimensions that are traced over
orderedDim = 1:totDim;
temp = orderedDim-tracingDim';
temp = ~sum(temp==0,1);
remainingDim = orderedDim(temp);

%Reform the vector to perform computation easily
psi = permute(psi,[tracingDim,remainingDim]);
psi = reshape(psi,[2^numel(tracingDim),2^numel(remainingDim)]);

%Prealocate reduced density matrix
densityMatrix = zeros(2^(numel(remainingDim)));

%Calculate the density matrix by having a single loop over the
    dimensions
%that are traced over
for i = 1:size(psi,1)
    densityMatrix = (double(densityMatrix))+(double(psi(i,:))).'*(
        double(conj(psi(i,:))));
end
end
```

D MATLAB: Correlation

Finally the code that is used to calculate the correlation between the different parts is given in this Appendix. The main part will consist of looping through all the lattice particles to compute the correlation for a pre-calculated vectorstate. The distance between the particles is calculated and the correlation is subsequently fitted as a function of distance with the periodically extended decaying exponential function. Next to the main part, the two function that used calculate the correlation as described in the theory, and calculate the distance by the L_1 metric.

The main part is:

```
clear; close all;
load('eigenvector_5x5_4000N')

%Initialising
M=5;N=5;
Corr = zeros(M*N,M*N);
pos = zeros(M*N,2);
CorrClean = reshape(Corr,[numel(Corr),1]);
distancesClean = reshape(distances,[numel(distances),1]);
vDistClean = reshape(vDist,[numel(vDist),1]);
hDistClean = reshape(hDist,[numel(hDist),1]);

%Calculate correlation between all the particles
for i=1:M*N
    for j=1:M*N
        Corr(i,j) = Correlation(PsiEigV_hil,i,j);
    end
end

%Determine the x and y position of particles in
pos(:,1) = M-mod(-(1:N*M),M);
pos(:,2) = ceil((1:N*M)/N);

%Determine total, vertical and horizontal distance
distances = Distance(pos,M,N);
vDist = abs(pos(:,1)-pos(:,1)');
hDist = abs(pos(:,2)-pos(:,2)');

%Ignore self-correlation
ignore = distancesClean==0;
distancesClean = distancesClean(not(ignore));
CorrClean = CorrClean(not(ignore));
vDistClean = vDistClean(not(ignore));
hDistClean = hDistClean(not(ignore));

plot(distancesClean,CorrClean,'.');

%Fit the periodically extended decaying exponential function
periodicAnsatz = @(a,xi,m,n,x,y) ...
    a*(exp(-y/xi)+2*cosh(-y/xi)*exp(-m/xi)/(1-exp(-m/xi))).*(exp(-x/xi
       )+2*cosh(-x/xi)*exp(-n/xi)/(1-exp(-n/xi)));
```

```
[periodicFit,gof] = fit([hDistClean,vDistClean],CorrClean,
    periodicAnsatz,'StartPoint',[1,1,1,1])
```

The function calculating the correlation and distance respectively:

```
function Corr = Correlation (Psi,i,j)
%%% Calculate the correlation for vectorstate Psi between particles i
    and j

%Note which dimensions are summed over to calculate the wanted state
    probability
numDim = numel(size(Psi));
sumDim = 1:numDim;
sumDim = sumDim(logical((sumDim~=i).*(sumDim~=j)));

%Calculate all the state probabilities
totalExp = abs(Psi).^2;

%Checking if there are enough particles, calculate the wanted state
%probability
if ~isempty(sumDim)
    spinExpectations = squeeze(sum(totalExp,sumDim));
else
    spinExpectations = totalExp;
end

%Use the state probability and the outcomes to compute the required
%expectation value in the definition of the correlation.
Corr = sum([1,-1;-1,1].*spinExpectations,'all')-sum([1,-1].*sum(
    spinExpectations,1))*sum([1;-1].*sum(spinExpectations,2));
end
```

```
function d = Distance(positions,M,N)
%%% Calculate the L1 distance
vDist = abs(positions(:,1)-positions(:,1)');
hDist = abs(positions(:,2)-positions(:,2)');
d = vDist+hDist;
end
```